Utp9p Facilitates Msn5p-mediated Nuclear Reexport of Retrograded tRNAs in *Saccharomyces cerevisiae*

Manoja B.K. Eswara, Andrew T. McGuire, Jacqueline B. Pierce, and Dev Mangroo

Department of Molecular and Cellular Biology, University of Guelph, Guelph, ON, N1G 2W1, Canada

Utp9p is a nucleolar protein that is part of a subcomplex containing several U3 snoRNA-associated proteins including Utp8p, which is a protein that shuttles aminoacyl-tRNAs from the nucleolus to the nuclear tRNA export receptors Los1p and Msn5p in *Saccharomyces cerevisiae*. Here we show that Utp9p is also an intranuclear component of the Msn5p-mediated nuclear tRNA export pathway. Depletion of Utp9p caused nuclear accumulation of mature tRNAs derived from intron-containing precursors, but not tRNAs made from intronless pre-tRNAs. Utp9p binds tRNA directly and saturably, and copurifies with Utp8p, Gsp1p, and Msn5p, but not with Los1p or aminoacyl-tRNA synthetases. Utp9p interacts directly with Utp8p, Gsp1p, and Msn5p in vitro. Furthermore, Gsp1p forms a complex with Msn5p and Utp9p in a tRNA-dependent manner. However, Utp9p does not shuttle between the nucleus and the cytoplasm. Because tRNA splicing occurs in the cytoplasm and the spliced tRNAs are retrograded back to the nucleus, we propose that Utp9p facilitates nuclear reexport of retrograded tRNAs. Moreover, the data suggest that Utp9p together with Utp8p translocate aminoacyl-tRNAs from the nucleolus to Msn5p and assist with formation of the Msn5p-tRNA-Gsp1p-GTP export complex.

INTRODUCTION

Trafficking of tRNA between the nucleus and cytoplasm is a complex process that plays an essential role in protein synthesis, regulation of cell division (Kruse *et al.*, 2000; White, 2004a,b; Ernens *et al.*, 2006; Ghavidel *et al.*, 2007), nutrient-related regulation of gene expression (Shaheen and Hopper, 2005, 2007; Hurto *et al.*, 2007; Whitney *et al.*, 2007), replication of the HIV genome (Zaitseva *et al.*, 2006), and neuronal development (Schmidt *et al.*, 2007). In eukaryotes, tRNAs are made as precursors that undergo a number of processing steps to become fully functional (Hopper and Phizicky, 2003). These steps involve removal of the 5'- and 3'-extensions, base modifications, addition of C, C, and A to their 3' ends, and removal of an intron for some tRNA species. For intronless pre-tRNAs, the maturation process occurs entirely in the nucleus in yeast, plants, and mammals (Hopper and Phizicky, 2003; Paushkin *et al.*, 2004; Englert *et al.*, 2007). Maturation of intron-containing pre-tRNAs occurs primarily in the nucleus; however, in *Saccharomyces cerevisiae* unlike in vertebrates and plants, the intron-containing precursors are exported to the cytoplasm for removal of the introns and the spliced tRNAs are returned to the nucleus for reasons that are not understood (Huh *et al.*, 2003; Yoshihisa *et al.*, 2003, 2007; Shaheen and Hopper, 2005; Takano *et al.*, 2005).

Although evidence reported suggests that nuclear import of spliced tRNAs occurs by a constitutive process (Takano *et al.*, 2005), the mechanism involved is poorly understood. Genetic studies have shown that inactivation of Rna1p blocks retrograde movement of tRNA when cells are starved of amino acids (Shaheen and Hopper, 2005). This suggests

that the Gsp1p-GTP/Gsp1p-GDP cycle plays a role in this process and that a β-karyopherin may facilitate nuclear import of tRNA. The β-karyopherin Mtr10p, which is involved in nuclear import of the RNA component of the *S. cerevisiae* telomerase, is also thought to play a role in retrograde movement of tRNA from the cytoplasm to the nucleus (Shaheen and Hopper, 2005). In contrast, other studies found that inactivation of Rna1p had no effect on nuclear import of tRNA in mutant cells lacking the function of the nuclear tRNA export receptors Los1p and Msn5p when grown in compete medium (Takano *et al.*, 2005). Furthermore, sodium azide or 2-dexoyglucose treatment of *msn5 los1* mutant cells was found to abolish nuclear import of tRNA (Takano *et al.*, 2005). These data suggest that nuclear import of tRNA requires energy and that ATP may be the energy source. Thus, there may be two retrograde pathways operating in yeast: one that is constitutive and dependent on ATP, and the other requiring the Gsp1p-GTP/Gsp1p-GDP cycle and operating in response to nutrient-related stress; interestingly, deprivation of rat hepatoma H4IIE cells of amino acids has been shown to result in retrograde movement of cytoplasmic tRNAs to the nucleus (Shaheen *et al.*, 2007).

The fully processed tRNAs from the two classes of precursor tRNAs are subjected to aminoacylation in the nucleus to ensure that they are functional before export to the cytoplasm (Lund and Dahlberg, 1998; Sarkar *et al.*, 1999; Grosshans *et al.*, 2000; Azad *et al.*, 2001; Steiner-Mosonyi and Mangroo, 2004). In *S. cerevisiae*, the tRNA aminoacylation quality assurance step has been shown to occur in the nucleolus (Steiner-Mosonyi and Mangroo, 2004). However, it is not known whether nuclear tRNA aminoacylation occurs in the nucleolus of other eukaryotes including mammals. tRNAs deemed functional in *S. cerevisiae* are picked up in the nucleolus by Utp8p and delivered to Los1p and Msn5p for translocation across the nuclear pore complex (NPC; Hellmuth *et al.*, 1998; Steiner-Mosonyi *et al.*, 2003; Takano *et al.*, 2005; Strub *et al.*, 2007). An unidentified protein

Table 1. Yeast strains used in this study

Strain	Genotype	Source
BY4741	*MATa, his3, leu2, met15, ura3*	Open Biosystems
UTP8-TAP	*MATa, his3, leu2, met15, ura3, UTP8::TAP-HIS3*	Open Biosystems
UTP9-TAP	*MATa, his3, leu2, met15, ura3, UTP9::TAP-HIS3*	Open Biosystems
UTP21-TAP	*MATa, his3, leu2, met15, ura3, UTP21::TAP-HIS3*	Open Biosystems
LOS1-TAP	*MATa, his3, leu2, met15, ura3, LOS1::TAP-HIS3*	Open Biosystems
MSN5-TAP	*MATa, his3, leu2, met15, ura3, MSN5::TAP-HIS3*	Open Biosystems
CCA1-TAP	*MATa, his3, leu2, met15, ura3, CCA1::TAP-HIS3*	Open Biosystems
MTR10-TAP	*MATa, his3, leu2, met15, ura3, MTR10::TAP-HIS3*	Open Biosystems
msn5	*MATa, his3, leu2, met15, ura3, msn5::KanMX6*	Open Biosystems
utp9-ts	*MATa, ura3, leu2, his3, can1::LEU2-MFA1pr::His3 utp9-ts::URA3*	Ben-Aroya *et al.* (2008)
utp8-ts	*MATa, ura3, leu2, his3, lys2, met15, can1::LEU2-MFA1pr::His3 utp8-ts::URA3*	Ben-Aroya *et al.* (2008)
W303	*MATa, ade2-1, ura3-1, his3-11, trp1-1, leu2-3, 112, can100*	ATCC
kar1-1	*MATα*	Shaheen and Hopper (2005)
YKL200	W303, *MATa, ade2-1, ura3-1, his3-1, trp1-1, leu2-3, can1-100, UBR1::GAL-HA-UBR1 (HIS3)*	Euroscarf
utp9-td	W303, *MATa, ade2-1, ura3-1, his3-11, trp1-1, leu2-3, can1-100, UBR1::GAL-HA-UBR1 (HIS3), YHR196w::CUP1-UBI4-myc-YHR196w (kanMX)*	Euroscarf
utp8-td	W303, *MATa, ade2-1, ura3-1, his3-11, trp1-1, leu2-3, can1-100, UBR1::GAL-HA-UBR1 (HIS3), YGR128c::CUP1-UBI4-myc-YGR128c (kanMX)*	This study
xpo1-1^{ts}	W303, *MATa, xpo1::LEU2, pRS313-xpo1-1^{ts}*	Stade *et al.* (1997)
rio2-1	*MATa his3 leu2 trp1 ura3 rio2::kanMX4, pRS315-rio2-1 (LEU)*	Schafer *et al.* (2003)
nmd3-2	*MATa trp1 his3 leu2 ura3 nmd3::kanMX4, pRS313-nmd3-2 (HIS)*	Gadal *et al.* (2001)
BY4743	*MATa/MATα; his3D1/his3D1, leu2D0/leu2D0, met15D0/MET15, LYS2/lys2D0, ura3D0/ura3D0*	Open Biosystems
utp8: P$_{GAL1}$-UTP8	Derivative of BY4743, *utp8::kanMX6, pRS416-GAL1-UTP8, MATa*	Steiner-Mosonyi *et al.* (2003)
utp10: P$_{GAL1}$-UTP10	Derivative of BY4743, *utp10::kanMX6, pRS416-GAL1-UTP10, MATα*	This study
utp13: P$_{GAL1}$-UTP13	Derivative of BY4743, *utp13::kanMX6, BG1805-GAL1-UTP13, MATa*	This study

is also responsible for movement of tRNAs across the NPC in *S. cerevisiae* based on the finding that a *los1 msn5* mutant strain was not affected in growth or viability (Takano *et al.,* 2005). In mammalian cells, translocation of tRNAs across the NPC is facilitated by Xpo-t and Xpo-5, the orthologues of Los1p and Msn5p, respectively (Kutay *et al.,* 1998; Arts *et al.,* 1998; Bohnsack *et al.,* 2002; Calado *et al.,* 2002). tRNAs arriving at the cytoplasmic side of the NPC in *S. cerevisiae* are collected and delivered to the translation apparatus by Cex1p (McGuire and Mangroo, 2007). This step in mammalian cells most likely involves Scyl1 the orthologue of Cex1p.

Although the overall mechanism of nuclear tRNA export is, in general, poorly understood, the details of specific steps are slowly emerging from studies carried out in both mammalian cells and *S. cerevisiae* to identify and characterize participants of the process. Recent biochemical studies in *S. cerevisiae* have provided evidence suggesting that Utp8p uses a channelling mechanism to collect aminoacyl-tRNAs from the aminoacyl-tRNA synthetases in the nucleolus and to deliver them to the nuclear tRNA export receptors located in the nucleoplasm and NPC (Strub *et al.,* 2007). However, the molecular mechanism by which Utp8p traffics tRNAs from the nucleolus to the export receptors is currently not known. Utp8p is a component of the U3 snoRNA-associated protein (Utp) complex involved in 18S rRNA biogenesis (Dragon *et al.,* 2002). Furthermore, Utp8p, Utp17p, Utp15p, Utp10p, Utp9p, Utp5p, and Utp4p of the Utp complex have been found to form a subcomplex involved in regulating transcription of the rRNA gene (Gallagher *et al.,* 2004; Krogan *et al.,* 2004). It is therefore possible that other Utp proteins of the subcomplex could also be playing a role in the trafficking of tRNAs from the nucleolus to the export receptors.

In this report we provide biochemical evidence that Msn5p is an authentic nuclear export receptor for tRNA in *S. cerevisiae*. Furthermore, we show that Utp9p is a nucleolar tRNA-binding protein that plays an intranuclear role that is essential for nuclear export of mature tRNAs derived from intron-containing pre-tRNAs, but not export of tRNAs derived from intronless pre-tRNAs. Moreover, nutrient stress conditions that block nuclear reexport of mature tRNAs derived from intron-containing pre-tRNAs had no effect on nuclear export of tRNAs made from intronless precursors. These results combined with the finding that Utp9p interacts with Msn5p but not with Los1p suggest that Utp9p participates in the reexport of retrograded tRNAs derived from intron-containing pre-tRNAs by the Msn5p-mediated nuclear tRNA export pathway. Furthermore, the data imply that Utp9p together with Utp8p translocate aminoacylated tRNAs from the nucleolus to Msn5p and assist with the formation of the Msn5p-tRNA-Gsp1p-GTP export complex.

MATERIALS AND METHODS

Strains and Plasmids

The *S. cerevisiae* strains used in this study are listed in Table 1. Plasmids pET19b and pET23d were purchased from Novagen (San Diego, CA). The pGEX-GST-TEV plasmid was obtained from Dr. D. Heinrichs (University of Western Ontario, Canada). pGEX-4T-GSP1 and pGEX-GSP1p (Q71L) were provided by Dr. U. Stochaj (McGill University, Montreal, Canada). pET28GST-LIC was obtained from the Structural Genomics Consortium (Toronto, Canada). pET9D-5S, pRS315-RPL25-GFP, and pRS316-RPS2-GFP were obtained from Dr. E. Hurt (University of Heidelberg, Germany). The BG1805-GAL1-UTP13 plasmid was obtained from Open Biosystems (Huntsville, AL). pCEN-URA-GAL1-UTP10 was prepared by introducing the UTP10 open reading frame (ORF), obtained by PCR amplification of *S. cerevisiae* genomic DNA, into the XhoI site of pRS416-CEN-URA-GAL1. The plasmid pET19-UTP9 was constructed by inserting the UTP9 ORF into the NdeI and BamHI sites of pET19b. The UTP9 ORF obtained by PCR using *S. cerevisiae* genomic DNA was cloned into the BseRI site of pET28GST-LIC by ligation-independent cloning using the In-Fusion PCR Cloning kit from Clontech Laboratories (Palo Alto, CA). The plasmids pET23d-MSN5, pGEX-LOS1, pGEX-TYS1, pET19-UTP8, pGEX-UTP8, and pET19b-GSP1 were described previously (Strub *et al.,* 2007). pET19b-GSP1 Q71L was prepared by obtaining the GSP1 ORF containing the Q71L mutation by PCR using pGEX-GSP1 (Q71L) as the template and cloning into the NdeI and BamHI sites of pET19b.

Generation of utp8-td

The *utp8-td* strain was generated using a one-step PCR approach as described (Kanemaki *et al.,* 2003). Briefly, a PCR product was generated using 70-mer primers that contain 50 bases at the 5′-end corresponding to sequences at the end of the UTP8 ORF and promoter region, and 20 bases at the 3′-end corresponding to sequences specific to the degron cassette using pKL187 plasmid (Euroscarf, Frankfurt, Germany) as the template. The PCR product was transformed into the diploid YMK165 strain (Euroscarf) containing one copy of *UBR1::HIS3* under the control of the *GAL1* promoter. The transformed diploid strain was sporulated in the presence of 0.1 mM CuSO$_4$ and screened for haploids containing the *HIS3* and *KanMX6* markers. Integration of the degron cassette into the N-terminus of *UTP8* was confirmed by PCR using primers specific to the degron cassette and the UTP8 ORF. Expression of the fusion protein was confirmed by Western blotting analysis using anti-Myc tag (Cell Signaling Technology, Beverly, MA) and anti-Utp8p antibodies.

Overexpression and Purification of His-tagged Proteins

Escherichia coli BL21 (DE3) Codon Plus RIL (Novagen) with pET19b-UTP9, pET19b-UTP8, pET19b-GSP1, or pET23d-MSN5 was grown in 1 l of 2YT broth containing 100 μg/ml ampicillin and 34 μg/ml chloramphenicol at 37°C to an A$_{600}$ of 0.4. The cultures were shifted to 15°C and expression of the His-tagged proteins was induced with 200–500 μM isopropyl β-D-thiogalactoside (IPTG) for 16 h. The cells were collected by centrifugation and resuspended in 30 ml of binding buffer: 20 mM NaH$_2$PO$_4$, pH 7.5, buffer containing 500 mM NaCl, 5 mM imidazole, 10 μg/ml RNase A and a mixture of protease inhibitors (Complete EDTA-free; Roche Applied Science, Indianapolis, IN). The cells were lysed at 70,000 kPa using a French press, and the lysate was clarified by centrifugation at 27,000 × g for 30 min. The clarified lysate was applied onto a 1 ml HisTrap HP column (GE Healthcare, Little Chalfont, Buckinghamshire, United Kingdom). The column was washed with 20 ml of 20 mM NaH$_2$PO$_4$, pH 7.5, buffer containing 500 mM NaCl and 50 mM imidazole and then with 20 mM NaH$_2$PO$_4$, pH 7.5, buffer containing 500 mM KCl to remove tRNA. The His-tagged proteins were eluted using a gradient of increasing concentration of imidazole in 20 mM NaH$_2$PO$_4$, pH 7.5, buffer containing 500 mM NaCl. Fractions containing purified protein were pooled and dialyzed against IPP150 buffer (25 mM Tris-HCl, pH 7.5, containing 150 mM NaCl, 20% glycerol [wt/vol], and 0.1% Nonidet P-40 [vol/vol]). The protein was concentrated and stored at −80°C. Utp9p-His was further purified by ion exchange chromatography using a HiTrap Q HP Sepharose column (GE Healthcare). HisTrap HP eluate containing Utp9p-His was dialyzed against 20 mM Tris-HCl, pH 7.5, buffer containing 100 mM NaCl and applied onto the HiTrap Q HP column. The column was eluted with a gradient of increasing concentration of NaCl up to 500 mM NaCl. Fractions containing purified protein were pooled and dialyzed against IPP150 and stored at −80°C after concentration. An aliquot of the concentrated proteins were subjected to phenol-chloroform extraction and RNA precipitation, and analyzed on a 2% agarose gel to check for the presence of tRNA. tRNA could not be detected with any of the purified proteins.

Overexpression and Purification of GST-tagged Proteins

E. coli BL21 (DE3) Codon Plus RIL (Novagen) containing pGEX-LOS1, pGEX-TYS1, or pGEX-UTP8 was grown in 1 l of 2YT medium containing 100 μg/ml ampicillin and 34 μg/ml chloramphenicol at 37°C to an A$_{600}$ of 0.4. *E. coli* BL21 (DE3) Codon Plus RIL containing pET28GST-LIC-UTP9 was grown in the presence of 100 μg/ml kanamycin and 34 μg/ml chloramphenicol. The cultures were shifted to 15°C, and protein expression was induced using 0.2–1 mM IPTG for 16 h. The cells were collected by centrifugation and resuspended in 30 ml of binding buffer (10 mM Na$_2$HPO$_4$ and 1.8 mM KH$_2$PO$_4$, pH 7.3, containing 140 mM NaCl, 2.7 mM KCl, 1 mM dithiothreitol [DTT]), a mixture of protease inhibitors (Complete EDTA-free; Roche Applied Science), and 10 μg/ml RNase A. The cells were lysed by using a French pressure cell at 70,000 kPa, and the lysate was clarified by centrifugation at 27,000 × g for 30 min. The clarified lysate was applied onto a GSTrap column (GE Healthcare). The column was washed with binding buffer and then with 20 mM NaH$_2$PO$_4$, pH 7.5, buffer containing 500 mM KCl to remove tRNA. The glutathione *S*-transferase (GST)-tagged protein was eluted using 50 mM Tris-HCl, pH 8.0, buffer containing 10 mM reduced glutathione and 1 mM DTT. The eluates were dialyzed against IPP150 buffer and stored at −80°C. GST-Utp8p was further purified by ion exchange chromatography using a HiTrap Q HP Sepharose column (GE Healthcare). GSTrap eluate containing GST-Utp8p was dialyzed against 20 mM Tris-HCl, pH 7.5, buffer containing 100 mM NaCl and applied onto the HiTrap Q HP column. The column was eluted with a gradient of increasing concentration of NaCl up to 500 mM NaCl. Fractions containing purified protein were pooled and dialyzed against IPP150 and stored at −80°C after concentration. An aliquot of the concentrated proteins were subjected to phenol-chloroform extraction and RNA precipitation, and analyzed on a 2% agarose gel to check for the presence of tRNA. tRNA could not be detected with any of the purified proteins.

Fluorescence In Situ Hybridization Analysis

The *utp9-td, utp8-td,* and YKL200 strains were grown at 23°C in YPD medium supplemented with 0.1 mM CuSO$_4$ to an A$_{600}$ of 0.6–0.7. The cells were

washed with water and shifted to YPG medium supplemented with 0.1 mM CuSO$_4$ and grown at 23°C for 6 h. The cells were washed and shifted to YPG medium without CuSO$_4$ and grown at 37°C for 1–6 h. The temperature-sensitive strains (*utp8-ts* and *utp9-ts*) were grown in YPD medium at 23°C to an A$_{600}$ of 0.6; the cells were diluted to an A$_{600}$ of 0.1 in YPD medium and grown at 37°C for 1–9 h. Fifty milliliters of culture was fixed and permeabilized as described (Grosshans *et al.,* 2000; Steiner-Mosonyi and Mangroo, 2004) and incubated at 37°C for 1 h in hybridization buffer (4× SSC, 50% formamide, 10% dextran sulfate, 125 μg/ml *E. coli* 5S rRNA, 500 μg/ml salmon sperm DNA, 0.5 U/μl RNasin, 10 mM DTT, and 1× Denhardt's). Hybridization was carried out at 37°C for 12 h in hybridization buffer containing 0.5 pmol/μl 5′-end Cy3-labeled oligonucleotide or 5′-end Alexa488-labeled oligo-dT. The cells were washed once for 5 min at room temperature with 2× SSC, two times with 1× SSC, and once with 0.5× SSC. DAPI (1 μg/ml) was used to visualize nuclear DNA. The slides were viewed under a 100× objective lens of a Nikon Eclipse 6600 microscope (Melville, NY). The images were recorded using a Coolsnapfx monochrome CCD digital camera (Roper Scientific, Tucson, AZ) and processed using Metamorph (Universal Imaging, West Chester, PA).

Oligonucleotides Used in This Study

The cellular location of mature tRNA^{Tyr}, tRNA^{Gly}, tRNA^{His}, and tRNA^{Leu} was detected using 5′-GCGAGTCGAACGCCCGATCTCAAGATTTACAGTCTTGC-GCCTTAAACCAACTTGGCTACC-3′, 5′-GGCCCAACGATGGCAACG-3′, 5′-TC-CTAGAATCGAACCAGGGTTTCATCGGCCACAACGATGTGTACTAACCAC-TATACTAAG-3′, and 5′-GCATCTTACGATACCTGAGCTTGAATCAGGCGC-3′, respectively. tRNA^{Trp} was detected using 5′-AACCTGCAACCCTTCGA-3′. This oligonucleotide hybridizes to all the different processing forms of tRNA^{Trp}. The 18S and 25S rRNAs were detected using 5′-CATGGCTTA-ATCTTTGAGAC-3′ and 5′-CTCCGCTTATTGATATGC-3′, respectively. mRNA was detected with a 30-mer poly-dT oligonucleotide.

Tandem Affinity Purification

Tandem affinity purification (TAP)-tagged strains were grown in 2 l of YPD medium to an A$_{600}$ of 2.0 at 30°C. The cells were harvested by centrifugation, resuspended in 50 ml of NP-40 buffer (15 mM Na$_2$HPO$_4$, pH 7.2, buffer containing 10 mM NaH$_2$PO$_4$, 2% NP-40 [vol/vol], 150 mM NaCl, 2 mM EDTA, 50 mM NaF, 0.1 mM Na$_3$VO$_4$, and protease inhibitors) and lysed using glass beads at 4°C. The lysate was clarified by ultracentrifugation at 142,000 × g for 75 min at 4°C and subjected to sequential affinity purification using IgG-Sepharose (GE Healthcare) and calmodulin-Sepharose as described (Puig *et al.,* 2001). The proteins in the final eluate were precipitated using 25% trichloroacetic acid, solubilized in LDS sample buffer (Invitrogen, Carlsbad, CA) and separated on 4–12% Novex Bis-Tris gels (Invitrogen). The separated proteins were transferred electrophoretically to Immobilon PVDF membrane (Millipore, Bedford, MA) and probed with rabbit anti-Utp9p, anti-Utp8p, anti-human TysRS, anti-Cex1p, anti-Los1p, anti-Gsp1p, or mouse anti-human eEF-1A (Upstate Cell Signaling, Waltham, MA).

Protein Extraction and Western Blot Analysis to Monitor Protein Degradation

utp9-td, utp8-td, and the parental YKL200 strain were grown as above and shifted to YPG medium without CuSO$_4$ and grown at 37°C for 1–3 h. Three milliliters of culture was pelleted, and the cell pellet was resuspended in breaking buffer (50 mM sodium phosphate, pH 7.4, 1 mM EDTA, 5% glycerol, and 1 mM PMSF). The cells were lysed using glass beads and clarified by centrifugation. An aliquot of the cell lysate was subjected to PAGE using a 4–12% Novex Bis-Tris gel, and the separated proteins were transferred to Immobilon-P PVDF membranes. Degradation of the target proteins was monitored by probing the membranes with anti-Utp9p, anti-Utp8p, or anti-Myc tag (Cell Signaling Technology). Expression of Ubr1p was monitored by probing the membranes with anti-hemagglutinin (HA) antibodies (Sigma-Aldrich, St. Louis, MO). The membranes were probed with anti-actin antibodies to confirm uniform loading of the samples.

Northern Hybridization Analysis

The *utp9-td* and YKL200 strains were grown at 23°C in YPD medium supplemented with 0.1 mM CuSO$_4$ to an A$_{600}$ of 0.6–0.7. The cells were washed with water and shifted to YPG supplemented with 0.1 mM CuSO$_4$ and grown at 23°C for 6 h. The cells were washed and shifted to YPG medium without CuSO$_4$ and grown at 37°C for 1–6 h. The cells were collected and total RNA was isolated using glass beads as described (Cleary and Mangroo, 2000). For analysis of tRNA processing and maturation, 2.5 μg of total RNA was separated on a 10% polyacrylamide gel containing 8 M urea using 1× TBE at room temperature. For analysis of the processing of rRNA, 2.5 μg of total RNA was separated on a 1.2% formaldehyde-MOPS agarose gels using 1× MOPS at room temperature. The separated RNAs were transferred electrophoretically onto Nytran membrane (Whatman, Clifton, NJ). The membranes were incubated at 37°C for 4 h in prehybridization solution consisting of 4× SSPE (1× SSPE = 0.18 M NaCl, 10 mM NaH$_2$PO$_4$, and 1 mM Na$_2$EDTA), 250 μg/ml sheared and denatured salmon sperm DNA, 0.1% SDS, and 10× Denhardt's

solution (1× Denhardt's = 0.02% bovine serum albumin, 0.02% polyvinylpyrrolidone 40, and 0.02% Ficoll). Hybridization was performed overnight at 37°C in prehybridization solution containing 5'-end ^{32}P-labeled oligonucleotide (1–2 × 10^6 cpm/ml). The membranes were washed twice for 30 min at room temperature and once for 30 min at 38°C with 1× SSPE and 0.1% SDS and subjected to autoradiography.

Analysis of the Aminoacylation Status of tRNAs

The *utp9-td*, *utp8-td*, and YKL200 strains were grown at 23°C in YPD supplemented with 0.1 mM CuSO$_4$ to an A$_{600}$ of 0.6–0.7. The cells were washed with water and shifted to YPG medium supplemented with 0.1 mM CuSO$_4$ and grown at 23°C for 6 h. The cells were washed and shifted to YPG medium without CuSO$_4$ and grown at 37°C for 3 h. The cells were centrifuged and nuclear and postnuclear fractions were isolated as described (Steiner-Mosonyi and Mangroo, 2004). Total RNA from the nuclear and postnuclear fractions was separated by electrophoresis on a 6.5% polyacrylamide gel containing 8 M urea at 4°C using 100 mM sodium acetate buffer, pH 5.0, and transferred onto Nytran Plus membranes. Northern analysis was performed as described above. Deacylated tRNA marker was prepared by incubating nuclear and cytoplasmic RNA in 100 mM Tris-HCl, pH 9.5, at 37°C for 1 h.

Loading Gsp1p with [γ-^{32}P]GTP

[γ-^{32}P] GTP (65 μM, 6000Ci/mmol) and 140 μM GTP were incubated with 30 μM Gsp1p in PBSM (10 mM Na$_2$HPO$_4$, 1.75 mM KH$_2$PO$_4$, 137 mM NaCl, 5 mM KCl, and 0.5 mM MgCl$_2$, pH 7.4, containing 10% glycerol) containing 5 mM EDTA at room temperature. After 30 min, MgCl$_2$ was added to a concentration of 10 mM and placed on ice for 10 min (Lounsbury and Macara, 1997; Kutay *et al.*, 1998). The mixture was then passed through a G50 spin column preequilibrated with PBSM to remove unbound nucleotide. The amount of Gsp1p-GTP [γ-^{32}P] was determined by filtering an aliquot of the flow through fraction from the G50 resin through nitrocellulose membrane and determining the amount of radioactivity trapped on the membrane.

Heterokaryon Shuttling Assay

W303*a* cells transformed with pRS416-CEN-URA-GAL1-UTP9-GFP or pRS416-CEN-URA-GAL1-XPO1-GFP were grown in CS medium containing 2% galactose, 2% raffinose and lacking uracil to midlogarithmic phase at 30°C. Expression of the green fluorescent protein (GFP) proteins was repressed by shifting the cells to CS medium containing 2% dextrose (CSD) and lacking uracil for 1 h at 30°C. The donor cells were mixed with recipient *kar1-1α* cells grown in CSD medium and pelleted by centrifugation (Dilworth *et al.*, 2001; Steiner-Mosonyi *et al.*, 2003). The cell pellet was resuspended in CSD medium and incubated at room temperature for 30 min. An aliquot of the cells was placed on glass slides coated with CSD medium containing 2% agarose and sealed with a coverslip. The slides were incubated at room temperature and visualized at various times by direct fluorescence microscopy.

In Vitro Protein-binding Analyses

The GST fusion proteins Los1p, Tys1p, Utp9p, Utp8p, or GST were bound to glutathione (GT)-Sepharose in IPP150 buffer (25 mM Tris-HCl, pH 7.4, 150 mM NaCl, and 0.1% NP-40) containing a cocktail of protease inhibitors and 1 mM DTT at 4°C for 1 h. All washing steps were carried with IPP150 buffer, and when required, total yeast mature tRNA was provided at a 10-fold molar excess of the K_d of the protein. Binding was performed with a twofold molar excess of the interacting protein at 4°C. The GST-tagged proteins were eluted from the resin using TEV, thrombin or 10 mM reduced glutathione. The final eluates and unbound proteins in the washes were subjected to electrophoresis on 4–12% Novex Bis-Tris gels and transferred to Immobilon-P PVDF membranes. The proteins were detected by Western blot analysis followed by SYPRO Ruby staining of the blots.

Binding of Nucleotides to Gsp1p (Q71L) for In Vitro Protein-binding Analyses

Gsp1p (Q71L) was purified in a single step using Talon metal affinity chromatography. The purified protein was dialyzed against 25 mM Tris-HCl, pH 7.4, buffer containing 150 mM NaCl, and incubated with a 10-fold molar excess of GTP in 25 mM Tris-HCl, pH 7.4, containing 150 mM NaCl, 5 mM EDTA, and 1 mM DTT at room temperature for 30 min. Magnesium chloride was added to a final concentration of 10 mM, and the mix was incubated on ice for at least 15 min (Bischoff *et al.*, 1994, 1995). Unbound nucleotide was removed by passing the mix through G50 spin columns.

RNA-binding Analysis

Interaction of Utp9p with tRNA was determined by substrate-induced intrinsic fluorescence quenching of tryptophan residues (Steiner-Mosonyi *et al.*, 2003; McGuire and Mangroo, 2007). The analysis was performed in 20 mM HEPES, pH 7.4, buffer containing 100 mM NaCl, 0.25 μM Utp9p, and increasing amounts of mature yeast tRNA, 75-mer single-stranded DNA oligonucleotide, or *E. coli* 5S rRNA (1, 2, 4, 6.25, and 8 μM). The 5S rRNA was prepared by in vitro transcription of linearized pET9D-5S template using Ribomax kit

from Promega (Madison, WI). Control reactions lacking the protein and containing tRNA or oligonucleotide alone were prepared as above. The reaction mixtures were incubated for 1 h at 4°C, and tryptophan fluorescence was measured using a Photon Technology International spectrofluorimeter (Lawrenceville, NJ) with excitation and emission slits set to 4 nm and excitation and emission wavelengths of 295 and 334 nm, respectively. The fluorescence intensity of each sample was subtracted from that of the appropriate control reaction and expressed as a percent reduction of the fluorescence intensity obtained with Utp9p alone. Msn5p interaction with tRNA was performed as described for Utp9p.

Fluorescence In Situ Hybridization Analysis in Conditional Mutants of utp10 and utp13

The *utp10* pCEN-URA-GAL1-UTP10 and *utp13* GB1805-CEN-URA-GAL1-UTP13 strains were prepared by sporulation and tetrad dissections of heterozygous strains with pCEN-URA-GAL1-UTP10 and BG1805-CEN-URA-GAL1-UTP13, respectively. The *utp8* pCEN-URA-GAL1-UTP8 strain was described previously (Steiner-Mosonyi *et al.*, 2003). The strains were grown in CS medium containing 2% galactose and 200 μg/ml G418, and lacking uracil to an OD$_{600}$ of 0.6 at 30°C. The cells were washed and diluted in CS medium containing 2% dextrose and lacking uracil to an OD$_{600}$ of 0.1 and grown at 30°C for 6 h. The cells were fixed at the indicated time points, and fluorescence in situ hybridization (FISH) analysis was performed to monitor the distribution of mature tRNA^{Tyr} as described above.

Nuclear-Cytoplasmic Distribution of Ribosomal Subunits

The *nmd3-2* Rpl25-GFP and *rio2-1* Rps2-GFP strains were grown in CS medium containing 2% dextrose and lacking leucine or uracil, respectively at 23°C to an OD$_{600}$ of 0.6. The cells were diluted to an OD$_{600}$ of 0.3 in prewarmed medium and shifted to 37°C for 4 h. The cells were treated with DAPI (2 μg/ml) for 30 min and washed with 1× PBS. YKL200- and *utp9-td*–expressing Rpl25-GFP or Rps2-GFP were grown in CS medium containing 2% dextrose and lacking leucine or uracil, respectively, at 23°C to an OD$_{600}$ of 0.6. Expression of Ubr1p and depletion of Utp9p were induced as described earlier. The cells were treated with DAPI (2 μg/ml) stain for 30 min and washed with 1× PBS. Localization of Rpl25 and Rsp2 was monitored by fluorescence microscopy.

RESULTS

Loss of Utp9p Function Affects Nuclear Export of Mature tRNAs Derived from Intron-containing Pre-tRNAs But Not Export of tRNAs Obtained from Intronless Precursors

As part of our ongoing efforts to identify proteins that participate in nuclear tRNA export in *S. cerevisiae*, we focused on investigating whether Utp proteins of the Utp8p-containing subcomplex could be playing a role in the nuclear tRNA export process. The Utp protein chosen for investigation is Utp9p. It is an essential protein located in the nucleolus (Giaever *et al.*, 2002; Huh *et al.*, 2003), and like Utp8p, an orthologue of Utp9p is not found in higher eukaryotes by PSI-BLAST searches.

To test the possibility that Utp9p is involved in the nuclear tRNA export process, we investigated whether depletion of Utp9p affects nuclear-cytoplasmic tRNA trafficking. Because Utp9p is essential, this analysis was conducted using a conditional mutant strain of Utp9p (*utp9-td*). In this strain, the chromosomal gene of Utp9p is under the control of the copper-inducible *CUP1* promoter and is tagged at the 5'-end with a heat inducible degron cassette (Kanemaki *et al.*, 2003). The degron cassette consists of a mutant form of the mouse dihydrofolate reductase, which is stable at 23°C but denatures at 37°C, exposing lysine residues that are recognized by the ubiquitin-mediated proteosome degradation pathway. To control the degradation, the chromosomal *UBR1* gene encoding the yeast ubiquitin ligase is under the control of the *GAL1* promoter. Thus, depletion of Utp9p is achieved by repression of the *CUP1* promoter, induction of the expression of Ubr1p, and incubation of the cells at 37°C. This strategy is clearly capable of depleting Utp9p, because *utp9-td* did not grow at 37°C on YP medium containing galactose (YPG) and without copper (Supplemental Figure S1). Similarly, *utp8-td*, which was prepared for use as a
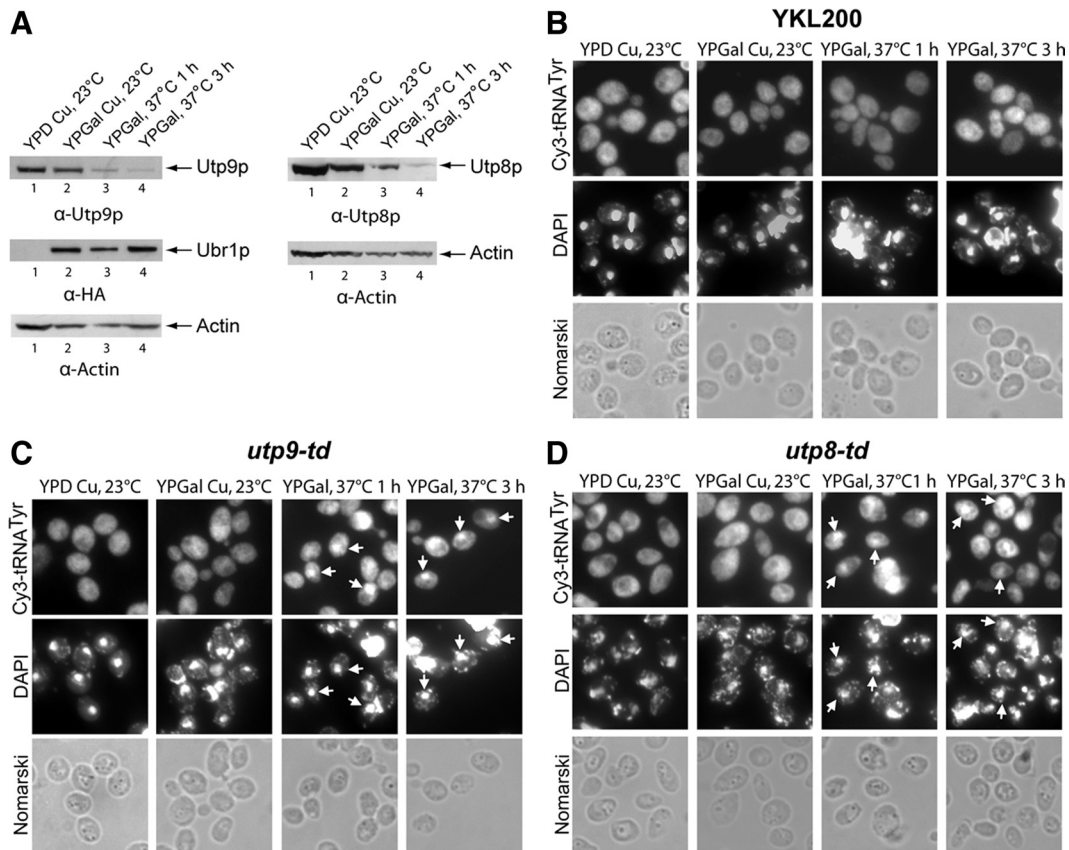
Figure 1. Depletion of Utp9p resulted in nuclear accumulation of tRNA^{Tyr}. The wild-type YKL200 strain, *utp9-td* and *utp8-td* were grown at 23°C in YPD medium supplemented with 0.1 mM CuSO$_4$. Expression of Ubr1p was then induced by growing the cells at 23°C for 6 h in YPG medium supplemented with 0.1 mM CuSO$_4$. Degradation of Utp9p or Utp8p was induced by growing the cells in YPG medium without CuSO$_4$ at 37°C for 1 and 3 h. Western blot analyses were performed to monitor the level of Utp9p (A, left), Ubr1p (A, left), actin (A) and Utp8p (A, right) in cell extracts prepared from *utp9-td* and *utp8-td* grown under the different conditions. The cellular location of tRNA^{Tyr} in YKL200 (B), *utp9-td* (C), and *utp8-td* (D) was monitored by FISH and the DNA was visualized by DAPI staining.

control, did not grow under these conditions (Supplemental Figure S1).

The time required to deplete Utp9p or Utp8p was determined by Western blot analyses. *utp9-td* (Figure 1A, left panel) and *utp8-td* (Figure 1A, right panel) were grown at 23°C in YP medium containing glucose (YPD) and copper (lane 1) and transferred to YPG medium with copper (lane 2) for 6 h at 23°C. The cells were then switched to YPG medium lacking copper and grown at 37°C for 1 (lane 3) or 3 h (lane 4). The level of actin was used to monitor the amount of cell extracts analyzed. The results indicate that Utp9p was maximally depleted within 1 h of incubation of *utp9-td* at 37°C in YPG medium lacking copper. In contrast, it took ~3 h to significantly decrease the level of Utp8p. Western blot analysis also indicate that depletion of the proteins coincide with the induced expression of Ubr1p (Figure 1A, left).

The effect of depletion of Utp9p on nuclear-cytoplasmic tRNA trafficking was assessed by using FISH to monitor the cellular location of tRNA^{Tyr}, a tRNA derived from intron-containing pre-tRNA. tRNA^{Tyr} was uniformly distributed in the wild-type isogenic YKL200 strain (Figure 1B), *utp9-td* (Figure 1C), and *utp8-td* (Figure 1D) grown in YPD medium with copper or YPG medium containing copper at 23°C. Furthermore, the nuclear-cytoplasmic distribution of tRNA^{Tyr} in YKL200 incubated at 37°C in YPG medium without copper for 1 or 3 h was not affected. In contrast, nuclear accumula-

tion of tRNA^{Tyr} was detected when Utp9p or Utp8p was depleted for 1 or 3 h.

To investigate whether nuclear accumulation of tRNA^{Tyr} was due specifically to the loss of Utp9p function or to degradation of a protein involved in nuclear tRNA export and associates with the degron-tagged Utp9p, nuclear-cytoplasmic trafficking of tRNA^{Tyr} was assessed in a temperature-sensitive mutant of Utp9p (Ben-Aroya *et al.*, 2008; Figure 2). FISH analyses indicate that the tRNA was distributed uniformly in the wild-type BY4741 strain (Figure 2A), *utp9-ts* (Figure 2B), *utp8-ts* (Figure 2C), and *XPO1* (Figure 2D) grown at 23°C. Nuclear accumulation of tRNA^{Tyr} was observed in *utp9-ts* and *utp8-ts*, but not in BY4741 incubated at 39°C for 3 h or *xpo1-1^{ts}* grown at 37°C for 3 h. Furthermore, tRNA^{Tyr} was detected in the nucleus of *utp9-ts* and *utp8-ts*, but not in BY4741 grown at 39°C for 6 or 9 h (Supplemental Figure S2). The data suggest that the nuclear accumulation of tRNA^{Tyr} observed in *utp9-td* was due specifically to the loss of Utp9p function.

To ascertain whether the Utp8p associated subcomplex is involved in nuclear tRNA export, the effect of depletion of Utp10p, which is a member of the subcomplex, on nuclear export of tRNA^{Tyr} was monitored. Furthermore, to exclude the possibility that depletion of any Utp protein will result in a defect in nuclear tRNA export, nuclear-cytoplasmic tRNA trafficking was investigated in a conditional mutant of
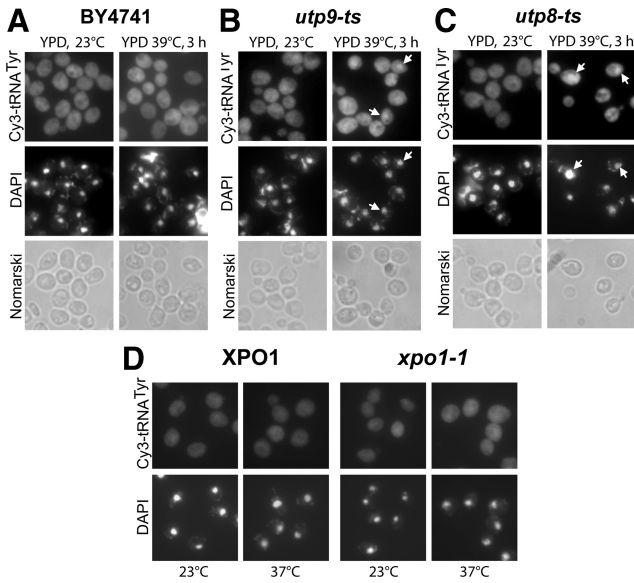
Figure 2. Loss of Utp9p function also caused nuclear accumulation of tRNA[Tyr] in a temperature-sensitive *utp9* mutant strain. The wild-type BY4741 strain (A), *utp9-ts* (B), and *utp8-ts* (C) were grown in YPD medium at 23°C and shifted to 39°C for 3 h. The W303 *XPO1* and *xpo1-1[ts]* strains (D) were grown at 23°C and shifted to 37°C for 3 h. The cellular location of tRNA[Tyr] was monitored by FISH and the DNA was visualized by DAPI staining.

Utp13p, a Utp protein that is not part of the Utp8p containing subcomplex. The wild-type BY4741 pCEN-URA-GAL1, *utp8* pCEN-URA-GAL1-UTP8, *utp10* pCEN-URA-GAL1-UTP10, or *utp13* BG1805-CEN-URA-GAL1-UTP13 strain was grown in CS medium containing galactose and then in CS medium containing dextrose for 6 h to repress expression of the Utp proteins (Figure 3). FISH analyses show that shifting the wild-type BY4741 strain (Figure 3A) from galactose to glucose did not affect nuclear export of tRNA[Tyr]. Similarly, the nuclear-cytoplasmic distribution of tRNA[Tyr] was not affected when Utp10p (Figure 3C) or Utp13p (Figure 3D) was depleted for 6 h. Furthermore, a defect in nuclear

tRNA export was not observed when Utp10p or Utp13p was depleted over a 9-h period (data not shown). However, loss of the function of Utp8p resulted in nuclear retention of tRNA[Tyr] (Figure 3B). These data suggest that only certain members of the Utp8p containing subcomplex are components of the *S. cerevisiae* nuclear tRNA export machinery.

Depletion of Utp9p has been shown to cause a marked decrease in transcription of the rRNA gene (Gallagher *et al.*, 2004). Northern blot analyses show that the levels of the 18S and 25S rRNAs decreased in total RNA isolated from *utp9-td* depleted of Utp9p over a 6-h period at 37°C (Supplemental Figure S3), which is consistent with previous reports (Gallagher *et al.*, 2004). Furthermore, the loss of Utp9p function appears to affect nuclear tRNA export and rRNA biogenesis concurrently. Thus, it is probable that the observed nuclear accumulation of tRNA[Tyr] when Utp9p was depleted could be due to a general effect on nuclear export processes caused by a defect in ribosome biogenesis. To exclude this possibility, the nuclear-cytoplasmic distribution of mRNA in *utp9-td* was compared with that in the temperature-sensitive strain of Xpo1p, which is a nuclear export receptor that influences nuclear mRNA export in *S. cerevisiae* (Stade *et al.*, 1997). FISH analyses show that mRNA was uniformly distributed in YKL200 (Figure 4A), *utp9-td* (Figure 4B) grown at 23°C in YPG (Figure 4), or YPD (Supplemental Figure S4) containing copper, and in *xpo1-1[ts]* (Figure 4C) incubated at 23°C. The nuclear-cytoplasmic distribution of mRNA was not affected in YKL200 incubated at 37°C for 1 h (Supplemental Figure S4) or 3 h (Figure 4). As expected, inactivation of Xpo1p in *xpo1-1[ts]* at 37°C for 3 h resulted in nuclear accumulation of mRNA (Stade *et al.*, 1997). However, depletion of Utp9p in *utp9-td* at 37°C for 1 (Supplemental Figure S4) or 3 h (Figure 4) had no effect on nuclear mRNA export.

To verify further that depletion of Utp9p does not have a general effect on nuclear export processes, nuclear export of the large and small ribosomal subunits was monitored in *utp9-td* (Figure 5). Rps2-GFP and Rpl25-GFP were used as markers to monitor nuclear export of the small and large ribosomal subunits, respectively. Fluorescence microscopy shows that Rps2-GFP was distributed uniformly in YKL200 (Figure 5A, middle column), *utp9-td* (right column), and
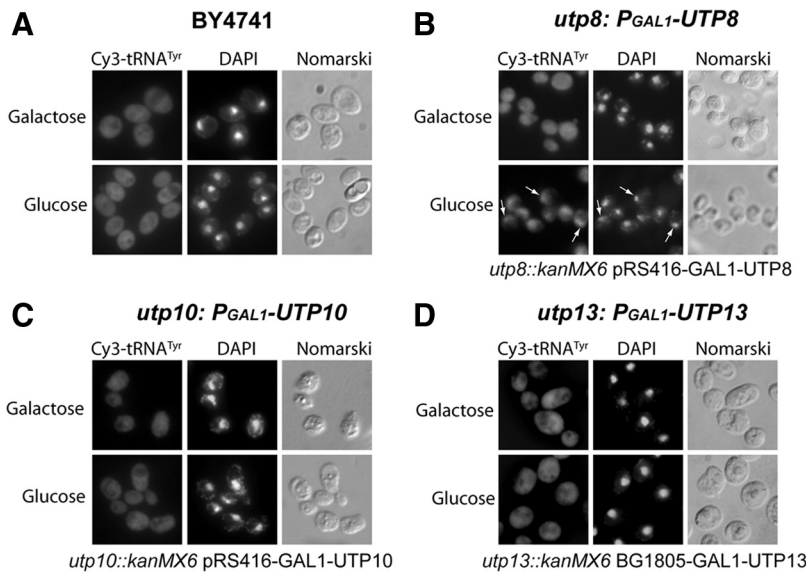

Figure 3. Depletion of Utp10p, a member of the Utp8p-containing subcomplex, or Utp13p, a Utp protein involved in 18S rRNA biogenesis does not affect nuclear tRNA export. The wild-type BY4741 strain harboring pCEN-URA-GAL1 (A), *utp8* pCEN-URA-GAL1-UTP8 (B), *utp10* pCEN-URA-GAL1-UTP10 (C), and *utp13* BG1805-CEN-URA-GAL1-UTP13 (D) were grown in CS medium containing 2% galactose and lacking uracil to A$_{600}$ of 0.6 at 30°C. The cells were washed and grown in CS medium containing 2% dextrose and lacking uracil at 30°C for 6 h. FISH was then used to monitor the nuclear-cytoplasmic distribution of tRNA[Tyr]. DNA was visualized by DAPI staining.
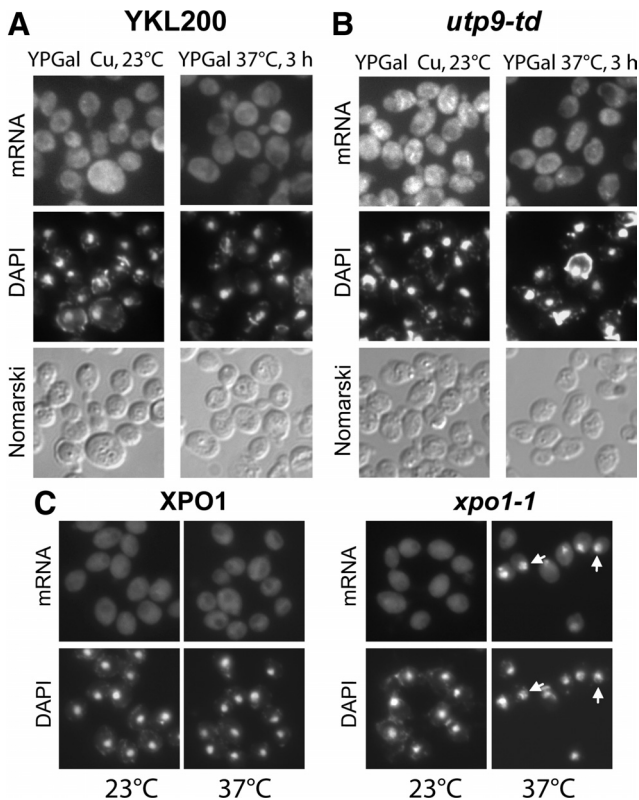
Figure 4. Depletion of Utp9p did not affect mRNA export. The wild-type YKL200 strain (A) and *utp9-td* (B) were grown at 23°C in YPD medium supplemented with 0.1 mM CuSO$_4$. Expression of Ubr1p was then induced by growing the cells in YPG medium supplemented with 0.1 mM CuSO$_4$ at 23°C for 6 h. Degradation of the Utp9p was induced by growing the cells in YPG medium without CuSO$_4$ at 37°C for 3 h. (C) The W303 *XPO1* and *xpo1-1^ts* strains were grown in YPD medium at 23°C and shifted to 37°C for 3 h. Nuclear-cytoplasmic distribution of mRNA was monitored by FISH using Alexa-488–labeled oligo-dT, and the DNA was visualized by DAPI staining.

rio2-1 (left column), a temperature-sensitive mutant that affects nuclear export of the small ribosomal subunit (Schafer *et al., 2003*), grown at 23°C. The nuclear-cytoplasmic distribution of Rsp2-GFP was not affected in YKL200 grown at 37°C or in *utp9-td* depleted of Utp9p for 3 h. As expected, loss of the function of Rio2p resulted in nuclear accumulation of Rsp2-GFP.

Rpl25-GFP was also found primarily in the cytoplasm in YKL200 (Figure 5B, middle column), *utp9-td* (right column), and *nmd3-2* (left column), a temperature-sensitive strain that affects nuclear export of the large ribosomal subunit (Gadal *et al., 2001*), grown at 23°C. However, a punctuate signal was observed in YKL200 and *utp9-td* but not in *nmd3-2* grown at 23°C. The distribution pattern of Rpl25-GFP was not affected in YKL200 grown at 37°C or in *utp9-td* depleted of Utp9p for 3 h. In contrast, nuclear retention of Rpl25-GFP was detected in *nmd3-2* grown at the nonpermissive temperature for 4 h. These data suggest that depletion of Utp9p does not affect nuclear export of the large and small ribosomal subunits. This is consistent with previous studies showing that depletion of Utp8p also did not affect nuclear export of the two ribosomal subunits (Steiner-Mosonyi *et al., 2003*). Moreover, the data taken together suggest that the loss of Utp9p function affects nuclear-cytoplasmic trafficking of tRNA specifi-

cally, and that this effect may be unrelated to the defect observed in rRNA biogenesis.

To ascertain whether depletion of Utp9p also affects nuclear export of mature tRNAs derived from intronless pre-tRNAs, the cellular location of tRNA^{Gly} in *utp9-td* and *utp9-ts* was investigated (Figure 6). Both tRNA^{Tyr}, which is made from intron-containing pre-tRNA (left panels), and tRNA^{Gly} (right panels) are distributed throughout the cells expressing Utp9p at 23°C (Figure 6 and Supplemental Figure S5). As observed before, tRNA^{Tyr} was retained in the nucleus of *utp9-td* and *utp9-ts* depleted of Utp9p (Figure 6, A and C, right and S5) for various times. In contrast, nuclear retention of tRNA^{Gly} was not observed when Utp9p was depleted in *utp9-td* for 1 (Supplemental Figure S5) or 3 h (Figure 6, B and D, right) at 37°C and in *utp9-ts* for 3 (Figure 6), 6 or 9 h (Supplemental Figure S5) at 39°C. The data show that Utp9p is only required for nuclear export of mature tRNAs derived from intron-containing pre-tRNAs. Furthermore, nuclear accumulation of tRNA^{Tyr} resulting from depletion of Utp9p was not caused by a defect in nuclear tRNA aminoacylation, which has been shown to affect the efficiency of nuclear tRNA export (Azad *et al., 2001*; Supplemental Figure S6) or tRNA splicing (Supplemental Figure S7). It is therefore possible that Utp9p participates in the reexport of mature tRNAs derived from tRNAs that were returned to the nucleus after undergoing splicing in the cytoplasm.

To test further that Utp9p is required for nuclear reexport of mature tRNAs derived from intron-containing pre-tRNAs, nuclear export of mature tRNA^{Leu} made from intron-containing pre-tRNA and mature tRNA^{His}, which is derived from intronless precursor was investigated in *utp9-td* (Figure 7). FISH analyses indicate that nuclear export of mature tRNA^{Leu} (Figure 7A) or tRNA^{His} (Figure 7B) was not affected in cells expressing Utp9p at 23°C. However, depletion of Utp9p in *utp9-td* at 37°C for 2 h results in nuclear retention of tRNA^{Leu} (Figure 7A, right) but not tRNA^{His} (Figure 7B, right). This data further establish that Utp9p participates in a pathway that is specific for nuclear export of mature tRNAs derived from intron-containing tRNAs.

Nitrogen or amino acid starvation of *S. cerevisiae* has been shown to cause nuclear accumulation of mature tRNAs derived from intron-containing pre-tRNAs (Shaheen and Hopper, 2005; Whitney *et al., 2007*). These observations led to the suggestion that nutrient deprivation blocks nuclear reexport of retrograded tRNAs. To test whether nutrient deprivation also blocks nuclear export of mature tRNAs that are made entirely in the nucleus by processing of intronless precursors, the cellular location of tRNA^{Gly} was monitored by FISH in cells starved of amino acids (top) or nitrogen (bottom). Starvation of *UTP9* of amino acids (Figure 8A) or nitrogen (bottom panels) for as little as 30 min results in nuclear accumulation of tRNA^{Tyr} (Figure 8, A and C) but not in accumulation of tRNA^{Gly} (Figure 8, B and D). Moreover, starvation of the cells for another 30 min did not affect nuclear-cytoplasmic trafficking of tRNA^{Gly}. Nuclear accumulation of tRNA^{Leu}, which is made from intron-containing pre-tRNA, but not tRNA^{His} derived from intronless precursor was also observed when the cells are deprived of amino acids (Supplemental Figure S8). The data show that amino acid or nitrogen deprivation only affects nuclear export of retrograded tRNAs, supporting the notion that Utp9p may be involved in reexport of retrograded tRNAs from the nucleus to the cytoplasm.
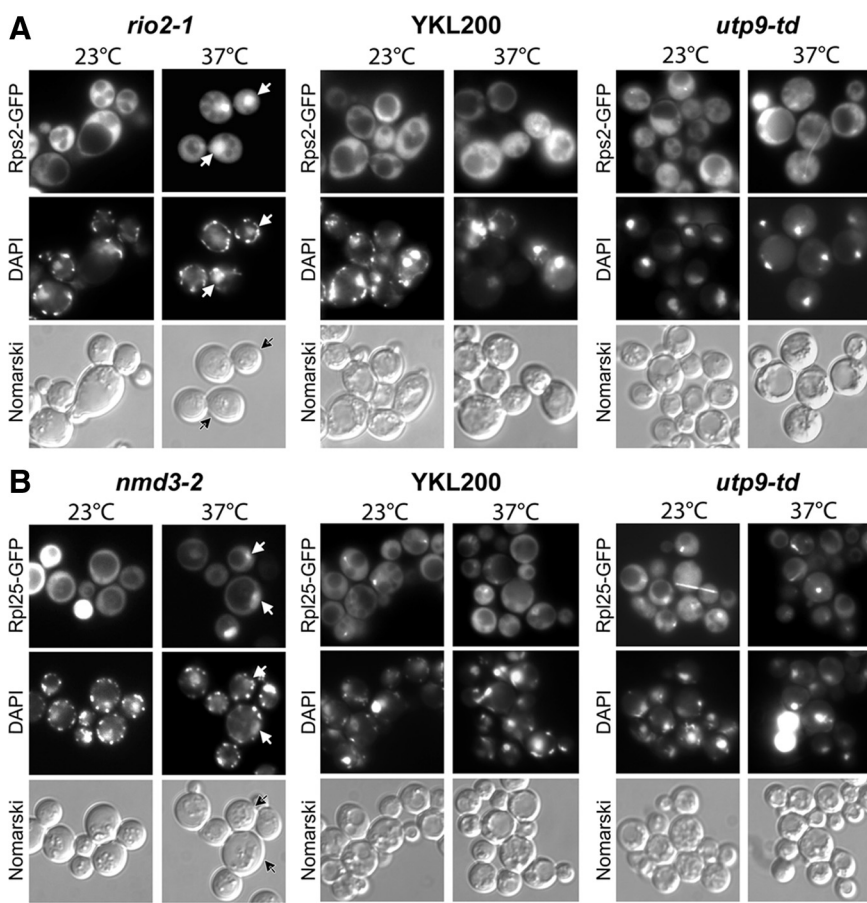
Figure 5. Depletion of Utp9p does not affect nuclear-cytoplasmic distribution of the large and small ribosomal subunits. Fluorescence microscopy was used to monitor the distribution of the small ribosomal subunit protein Rps2-GFP (A) in *rio2-1*, YKL200 and *utp9-td* and the large ribosomal subunit protein Rpl25-GFP (B) in *nmd3-2*, YKL200, and *utp9-td* at the permissive (23°C) and nonpermissive (37°C) temperatures. DAPI staining was performed to visualize the nucleus.

Utp9p Binds tRNA Directly and Saturably In Vitro But Does Not Function as a Nuclear tRNA Export Receptor

To understand how Utp9p influences nuclear-cytoplasmic trafficking of mature tRNAs made from intron-containing pre-tRNAs, the ability of Utp9p to interact with tRNA was determined using substrate-induced intrinsic fluorescence quenching of tryptophan residues (Figure 9). The analysis shows that recombinant Utp9p binds mature yeast tRNA directly and saturably (Figure 9A). The calculated affinity of Utp9p for tRNA is 2 μM. Utp9p also interacts with a 76-base pair DNA oligonucleotide (Figure 9B) and 5S rRNA (Figure 9C), but this binding was not saturable using the same concentrations used for tRNA binding. The data suggest that Utp9p has a tRNA-binding site, but it will bind nucleic acid nonspecifically in vitro. This behavior is commonly observed for bona fide prokaryotic and eukaryotic tRNA-binding proteins, including Utp8p, Cex1p, and Arc1p (Gite and RajBhandary, 1997; Wang and Schimmel, 1999; Steiner-Mosonyi *et al.,* 2003; McGuire and Mangroo, 2007; McGuire *et al.,* 2009). Thus, the data suggest that tRNA is a substrate for Utp9p in vivo.

Loss of the function of Los1p and Msn5p has been shown to affect the efficiency of nuclear tRNA export in *S. cerevisiae*, but not growth of the cells (Takano *et al.,* 2005). This led to the suggestion that an unidentified receptor is also involved in nuclear tRNA export. To ascertain whether Utp9p functions as a nuclear tRNA export receptor, a heterokaryon shuttling assay was used to investigate whether Utp9p shuttles between the nucleus and cytoplasm (Dilworth *et al.,* 2001; Steiner-Mosonyi *et al.,* 2003). Xpo1p, a nuclear receptor that is required for nuclear export of proteins with a leucine-rich nuclear export signal, was used as a control for a protein known to shuttle between the nucleus and cytoplasm (Stade *et al.,* 1997). The shuttling assay involves monitoring the movement of a protein from a donor nucleus to a recipient nucleus in heterokaryons. To avoid nuclear import of newly synthesized Utp9p and Xpo1p into the recipient nucleus, the donor strain harboring a low copy number plasmid with *UTP9-GFP* or *XPO1-GFP* under the control of the *GAL1* promoter was first grown in synthetic medium containing galactose to induce expression of the fusion proteins, and then briefly in medium containing glucose to repress the *GAL1* promoter. The donor strain was then mated with a *kar1-1* mutant strain, which is defective in nuclear fusion, on medium containing glucose. Movement of Utp9-GFP and Xpo1-GFP between nuclei was monitored by direct fluorescence microscopy (Figure 10). Utp9-GFP was found in a single nucleus in all heterokaryons analyzed over a 5-h period after mating was initiated (Figure 10A). In contrast, Xpo1-GFP was detected in both nuclei of heterokaryons over the same period (Figure 10B). The data suggest that Utp9p most likely does not function as an export receptor or an adaptor protein for a nuclear tRNA export receptor.

Utp9p Interacts with Utp8p But Not with Aminoacyl-tRNA Synthetases

TAP followed by mass spectrometric analyses have shown that Utp8p forms a complex with Utp17p, Utp15p, Utp10p, Utp9p, Utp5p, and Utp4p in vivo (Krogan *et al.,* 2004). We have also established by TAP and Western blot analyses using anti-Utp8p that Utp8p copurified with Utp17p, Utp15p, Utp10p, Utp9p, Utp5p, and Utp4p (data not
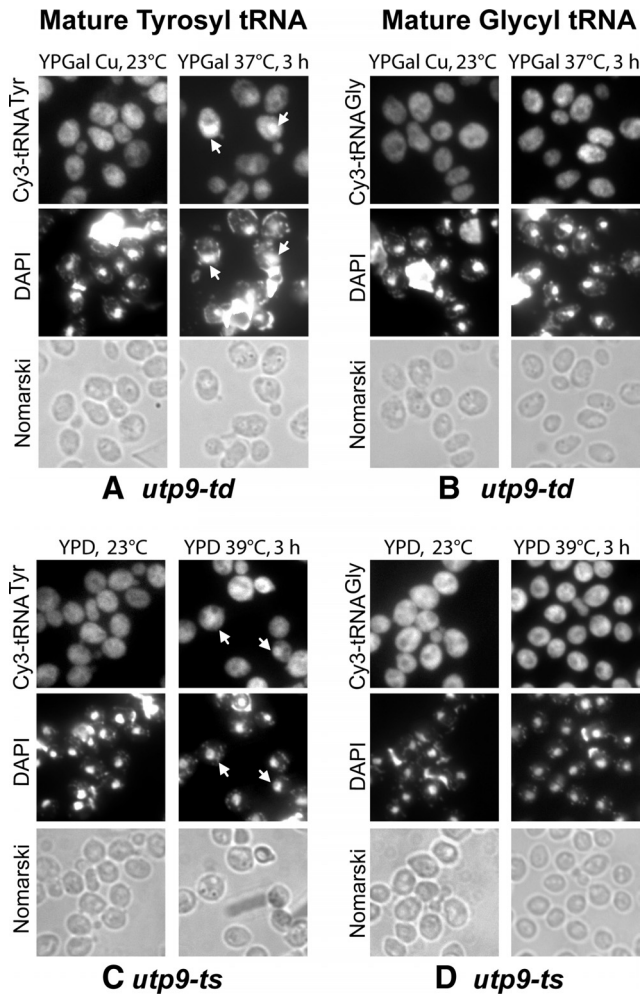
Figure 6. Loss of Utp9p function resulted in nuclear accumulation of mature tRNA^{Tyr} derived from intron-containing pre-tRNA but not mature tRNA^{Gly} obtained from intronless precursor. *utp9-td* (top panels) was grown at 23°C in YPD medium supplemented with 0.1 mM CuSO$_4$. Expression of Ubr1p was then induced by growing the cells in YPG medium supplemented with 0.1 mM CuSO$_4$ at 23°C for 6 h. Degradation of the Utp9p was induced by growing the cells in YPG medium without CuSO$_4$ at 37°C for 3 h. *utp9-ts* (bottom panels) was grown in YPD medium at 23°C and shifted to 39°C for 3 h. The cellular location of tRNA^{Tyr} (left panels) and tRNA^{Gly} (right panels) was detected by FISH and the DNA was visualized by DAPI staining.

Figure 7. Depletion of Utp9p results in nuclear accumulation of mature tRNA^{Leu} derived from intron-containing pre-tRNA but not mature tRNA^{His} obtained from intronless precursor. YKL200 (left panels) and *utp9-td* (right panels) were grown at 23°C in YPD medium supplemented with 0.1 mM CuSO$_4$. Expression of Ubr1p was then induced by growing the cells in YPG medium supplemented with 0.1 mM CuSO$_4$ at 23°C for 6 h. Degradation of the Utp9p was induced by growing the cells in YPG medium without CuSO$_4$ at 37°C for 2 h. The cellular location of tRNA^{Leu} (top panels) and tRNA^{His} (bottom panels) was detected by FISH and the DNA was visualized by DAPI staining.

shown). Furthermore, we have verified that Utp9p copurifies with Utp8-TAP by Western blot analysis (see TAP eluate in Figure 11A). The proteins that copurify with Utp8-TAP were also detected by SYPRO Ruby staining of the blot (Figure 11B). To ascertain whether Utp9p interacts directly with Utp8p, in vitro protein-binding studies were conducted (Figure 11C). GST-Utp8p bound to GT-Sepharose with (lane 3) or without (lane 4) tRNA and bound GST (lane 5) were incubated with a twofold molar excess of Utp9p. The resins were washed and GST-Utp8p was eluted with glutathione. Purified Utp9p (lane 1) and GST-Utp8p (lane 2), the bound proteins and unbound Utp9p in the wash eluates were subjected to Western blot analyses to detect Utp9p (top two rows) and Utp8p (middle row). Densitometric analyses of the blots indicate that the same amount of Utp9p interacts with Utp8p loaded with tRNA or free of tRNA (cf. lanes 3
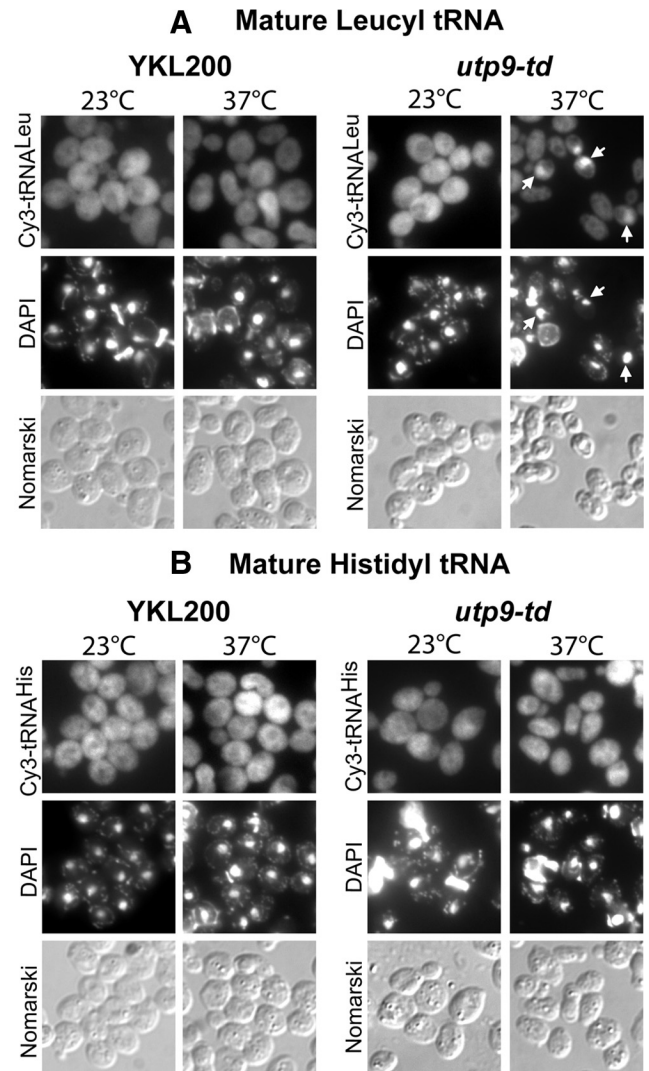
and 4). Furthermore, no interaction was detected between Utp9p and GST (lane 5). SYPRO Ruby staining of the blot also shows that Utp9p interacts with Utp8p in a tRNA-independent manner (bottom row), and that this interaction is fairly weak. The data suggest that Utp9p may act together with Utp8p to facilitate a step after the tRNAs have undergone aminoacylation in the nucleolus.

Utp8p was shown to interact with Tys1p by TAP and protein-binding studies in vitro (Strub *et al.*, 2007). Furthermore, this interaction was found to occur in the nucleolus using a split GFP system (Strub *et al.*, 2007). Therefore, TAP was used to ascertain whether Utp9p interacts with aminoacyl-tRNA synthetases in vivo by monitoring the tyrosyl-tRNA synthetase Tys1p (Figure 11A). Utp9-TAP was puri-
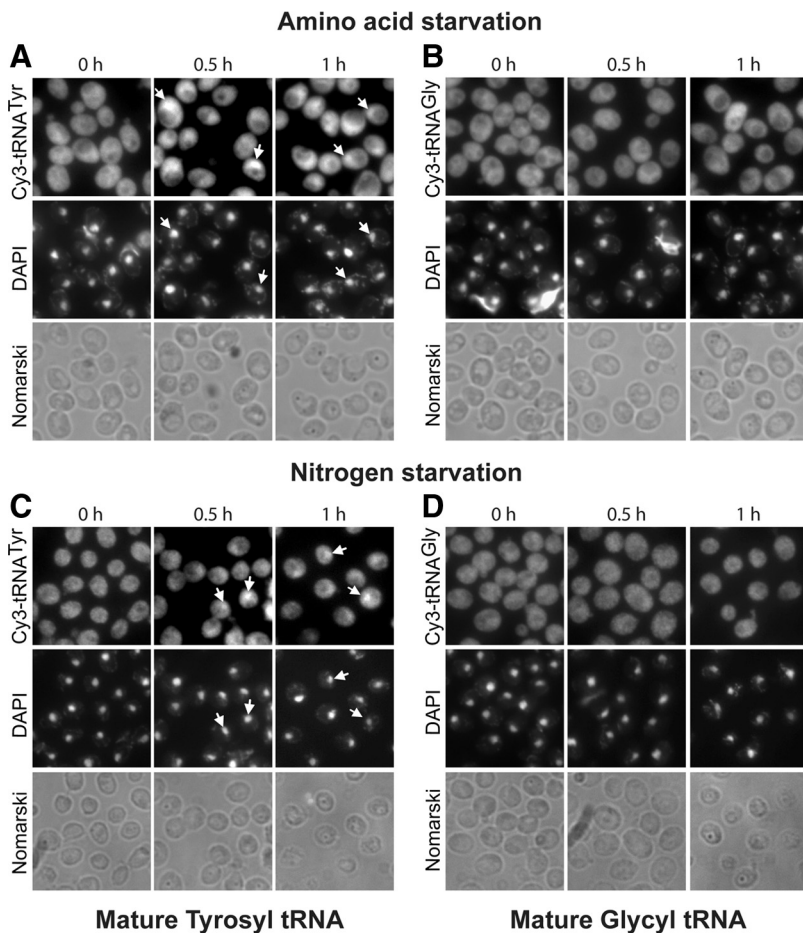
Amino acid starvation

Nitrogen starvation

Mature Tyrosyl tRNA   **Mature Glycyl tRNA**

Figure 8. Nutrient stress blocks nuclear export of retrograded mature tRNA obtained from intron-containing pre-tRNAs, but not export of mature tRNA made from intronless precursor. *S. cerevisiae* cells were starved of amino acids (top panels) or nitrogen (bottom panels) in synthetic medium containing glucose for the times indicated, and the cellular distribution of mature tRNA^{Tyr} (left panels) and tRNA^{Gly} (right panels) was monitored by FISH. The DNA was visualized by DAPI staining.

fied from cell extract prepared from *UTP9-TAP* by sequential chromatography on IgG-Sepharose and calmodulin-Sepharose. Western blot analysis detected Tys1p in the cell lysate (lane 1) and flow-through from the IgG-Sepharose resin (lane 2), but none was found in the final eluate from the calmodulin-Sepharose resin (TAP eluate; lane 3). The blot was then stained with SYPRO Ruby to detect the proteins that copurify with Utp9p (Figure 11B). In vitro protein-binding analyses also show that Utp9p did not interact with Tys1p in the absence or presence of tRNA (Supplemental Figure S9). The data suggest that Utp9p may not interact with Utp8p to collect aminoacyl-tRNAs from the aminoacyl-tRNA synthetases. Based on the function of Utp8p, it is possible that Utp9p interacts with Utp8p to translocate aminoacylated tRNAs out of the nucleolus and deliver them to the nuclear tRNA export receptors.

Utp9p May Deliver Retrograded tRNAs to Msn5p for Translocation across the NPC

To understand the role of Utp9p in tRNA export, TAP was conducted to determine whether Utp9p copurifies with the known and putative nuclear tRNA export receptors Los1p and Msn5p, respectively, and Cca1p, which is also thought to facilitate translocation of mature tRNA across the NPC. Lysates were prepared from cells expressing Msn5-TAP and Mtr10-TAP, which is a nuclear import receptor shown to be involved in nuclear tRNA import (Shaheen and Hopper, 2005), Cca1-TAP or Los1-TAP, and subjected to TAP using IgG-Sepharose and calmodulin-Sepharose. Aliquots of the

cell lysate (lane 1), proteins that did not bind to IgG-Sepharose (lane 2, flow-through), and proteins bound to calmodulin-Sepharose (lane 3) were subjected to Western blot analysis (Figure 12A), followed by SYPRO Ruby staining of the blots to detect the proteins directly (Figure 12C). Utp9p was detected in the cell lysate (lane 1) and the flow-through from the IgG-Sepharose resin (lane 2). In addition, Utp9p was found to copurify with Msn5p (lane 3) but not with Mtr10p, Cca1p, or Los1p.

TAP using cell extract prepared from cells expressing Utp9-TAP was also conducted to test whether Cex1p, a cytoplasmic component of the *S. cerevisiae* nuclear tRNA export process, or eukaryotic elongation factor eEF-1A, which delivers aminoacyl-tRNAs to the ribosomes, copurifies with Utp9p (Figure 12B). Western blot analyses detected Los1p, eEF-1A, and Cex1p in the cell lysate (lane 1) and IgG-Sepharose flow-through (lane 2). However, neither eEF-1A nor Cex1p copurified with Utp9-TAP (lane 3). As observed before, Los1p did not copurify with Utp9-TAP (lane 3). SYPRO Ruby staining of the blot (Figure 12C) shows that a number of proteins copurified with Utp9p. The data taken together indicate that Utp9p copurifies specifically with Msn5p.

To determine whether the interaction between Utp9p and Msn5p is direct, in vitro protein-binding studies were conducted (Figure 13A). GST-Utp9p bound to GT-Sepharose in the presence (lane 3) or absence (lane 4) of tRNA and bound GST (lane 5) were incubated with a twofold molar excess of Msn5p. The resins were washed, and Utp9p was released
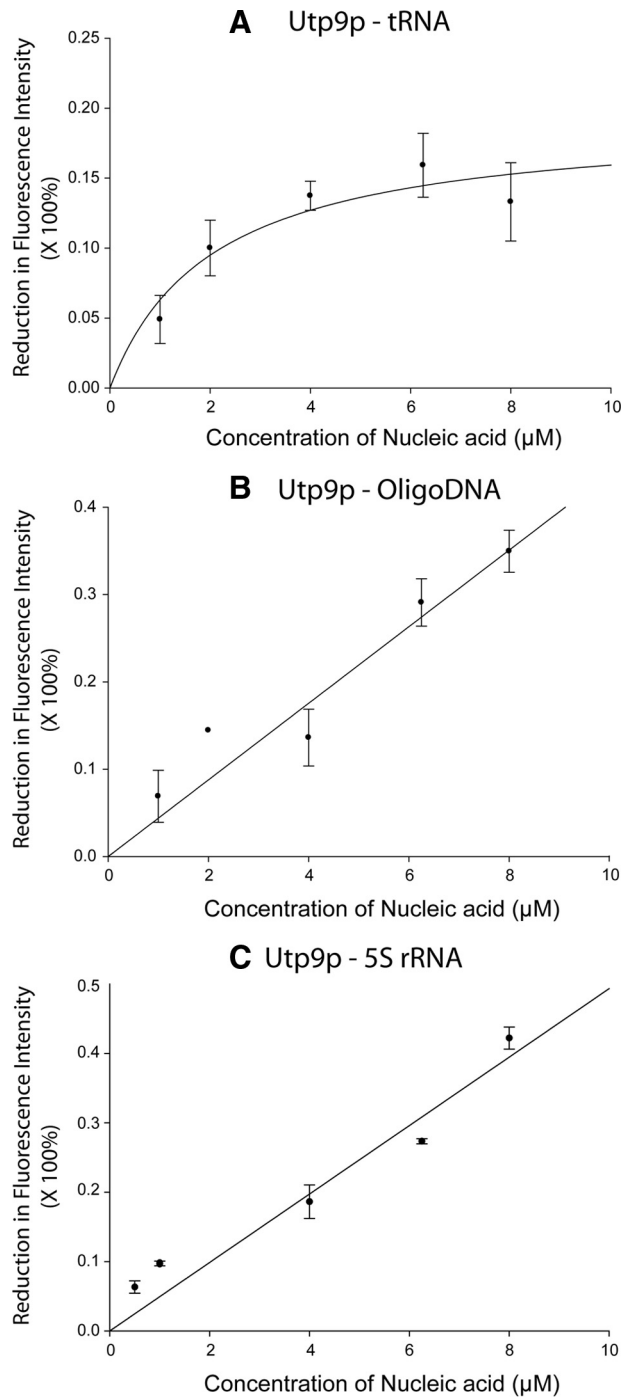
Figure 9. Utp9p binds tRNA directly and saturably. Substrate-induced intrinsic fluorescence quenching of Trp residues was used to determine whether Utp9p interacts with tRNA (A), DNA (B), or 5S rRNA (C).

Figure 10. Utp9p does not function as a nuclear tRNA export receptor. A heterokaryon shuttling assay was used to test whether Utp9p has the ability to shuttle between the nucleus and cytoplasm. Heterokaryons were identified by bright field microscopy and then analyzed for the location of Utp9-GFP (A) and Xpo1-GFP (B).

from GST using thrombin. Purified GST-Utp9p (lane 1) and Msn5p (lane 2), the bound proteins and unbound Msn5p in the wash eluates were subjected to Western blot analysis to monitor Msn5p (top panels) and Utp9p (middle panel). Utp9p was found to interact with Msn5p in the presence (lane 3) and absence (lane 4) of tRNA. However, Msn5p appears to interact better with Utp9p containing tRNA, because the amount of Msn5p bound to Utp9p loaded with
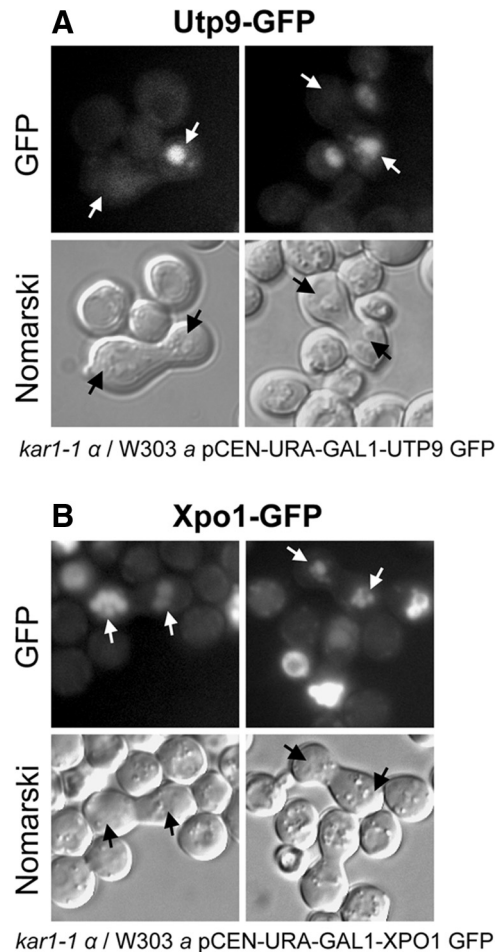
tRNA is ~1.5-fold higher compared with that bound to Utp9p free of tRNA (cf. lanes 3 and 4). In contrast, Msn5p did not interact with GST (lane 5). SYPRO Ruby staining of the blot indicates that only a small amount of Msn5p interacted with Utp9p, suggesting that the binding was weak irrespective of the presence or absence of tRNA (bottom panel).

To verify that the interaction between Msn5p and Utp9p is specific, Utp9p was tested for an association with Los1p in vitro (Figure 13B). GST-Los1p bound to GT-Sepharose in the presence (lane 3) or absence (lane 4) of tRNA and bound GST were incubated with a twofold molar excess of Utp9p. The resins were washed and Los1p was released from GST using TEV protease. Purified Utp9p (lane 1) and GST-Los1p (lane 2), the bound proteins and unbound Utp9p in the wash eluates were subjected to SDS-PAGE. Western blot analysis (top panel and middle panels), and SPYRO Ruby staining of the blot (bottom panel) were used to detect Utp9p (top panels) and Los1p (middle panel). Both analyses show that Utp9p did not interact with Los1p irrespective of the presence or absence of tRNA.

In addition to being the orthologue of the mammalian Xpo-5, genetic studies led to the suggestion that Msn5p functions as a nuclear tRNA export receptor (Takano *et al.*,
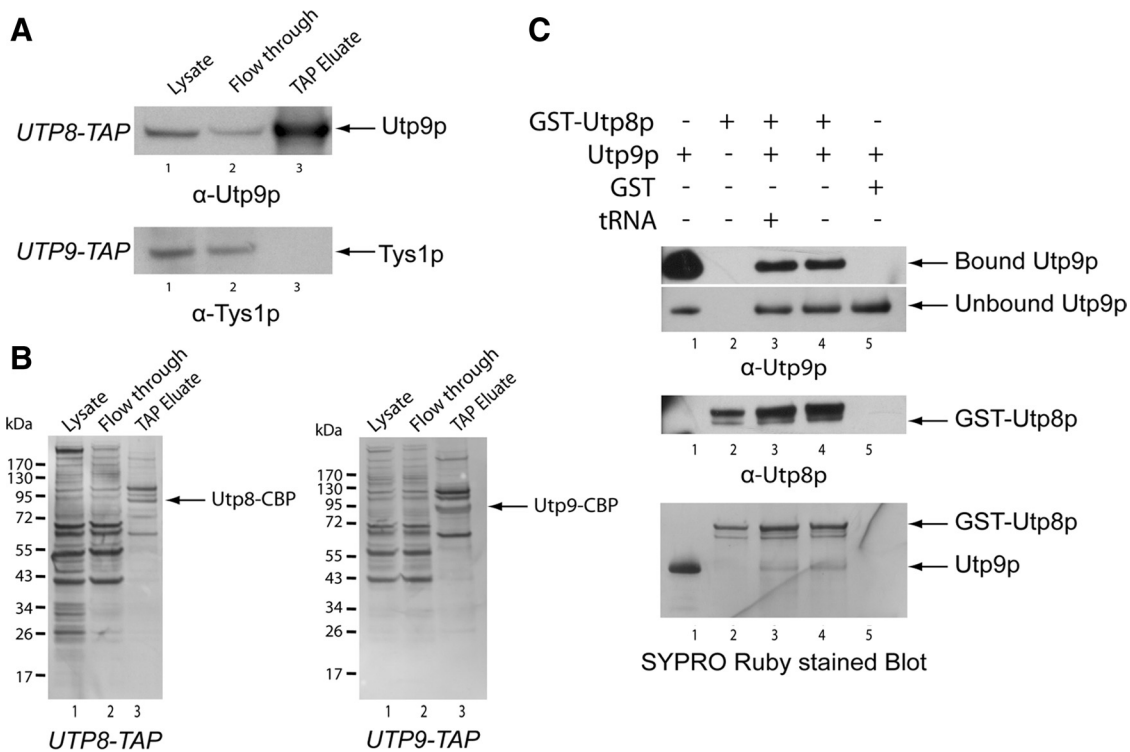
Figure 11. Utp9p interacts directly with Utp8p but not with aminoacyl-tRNA synthetases in vivo. Cell extract prepared from *UTP8-TAP* (top) or *UTP9-TAP* (bottom) was subjected to TAP using IgG-Sepharose and calmodulin-Sepharose. Utp9p or Tys1p in cell lysate (A, lane 1), the flow through from the IgG-Sepharose chromatography step (A, lane 2) and the eluate of proteins bound to calmodulin-Sepharose (TAP Eluate; A, lane 3) were detected by Western blot analysis. The blots were then stained with SYPRO Ruby to detect proteins that copurified with Utp8p and Utp9p, respectively (B). To test whether Utp9p interacts directly with Utp8p, GST-Utp8p (100 μg, 1 nmol) bound to GT-Sepharose in the presence (C, lane 3) or absence (C, lane 4) of 6 μM tRNA was incubated with a twofold molar excess of Utp9p (130 μg, 2 nmol). The same amount of Utp9p was incubated with bound GST (C, lane 5). The resins were washed and eluted with 10 mM glutathione. Purified Utp9p (lane 1) and GST-Utp8p (lane 2), the bound proteins, and unbound Utp9p in wash eluates were subjected to Western blot analyses to detect Utp9p (top panels) and GST-Utp8p (middle panel), followed by SYPRO Ruby staining of the blot (bottom panel).

2005), and this notion is consistent with in vitro and in vivo studies showing that Msn5p interacts with Utp8p and Cex1p (McGuire and Mangroo, 2007; Strub *et al.*, 2007). However, biochemical evidence verifying that Msn5p is a nuclear tRNA export receptor has not been reported. The use of substrate-induced intrinsic fluorescence quenching of tryptophan residues to test whether Msn5p is capable of interacting with tRNA shows that it binds tRNA nonsaturably with a calculated K_d of 753 μM (Figure 14A). The data suggest that Msn5p is interacting nonspecifically with the tRNA, because this method has been used to show that Utp8p, Cex1p, and Utp9p bind tRNA saturably and with very good affinity (Figure 9; Steiner-Mosonyi *et al.*, 2003; McGuire and Mangroo, 2007).

Like other β-karyopherin export receptors including the nuclear tRNA export receptor Los1p, loading of Msn5p with protein cargo has been shown to be dependent on the Ran GTPase Gsp1p in the GTP bound form (Hellmuth *et al.*, 1998; Quan *et al.*, 2006). Consequently, protein-binding studies were conducted in vitro to ascertain whether the interaction between Msn5p and tRNA is dependent on Gsp1p-GTP (Figure 14B). For this analysis the Gsp1p (Q71L) mutant was used, because it is unable to hydrolyze GTP (Maurer *et al.*, 2001; Quan *et al.*, 2006). GST-Msn5p bound to GT-Sepharose was incubated in the presence (lane 3) or absence (lane 4) of tRNA and in the presence of a twofold molar excess of Gsp1p (Q71L) loaded with GTP. The same amount of Gsp1p (Q71L) was incubated with bound GST (lane 5). The resins

were washed and GST-Msn5p was released using glutathione. Purified Gsp1p (Q71L; lane 1) and GST-Msn5p (lane 2), the bound proteins, and unbound Gsp1p in the wash eluates were subjected to Western blot analyses to detect Gsp1p (top panels) and GST-Msn5p (middle panel). Gsp1p (Q71L) was found to interact with Msn5p in the presence (lane 3) or absence (lane 4) of tRNA, but not with bound GST (lane 5). A smaller amount of Gsp1p was bound to Msn5p in the absence of tRNA compared with that bound to Msn5p in the presence of tRNA. However, this reduction in Gsp1p binding in the absence of tRNA is due to less GST-Msn5p bound to the resin. Quantification by densitometric analyses of the blots indicate that the same amount of Gsp1p was bound to Msn5p in the absence or presence of tRNA (cf. lanes 3 and 4). Thus, the interaction between Msn5p and Gsp1p occurs independently of tRNA. SYPRO Ruby staining of the blot (bottom panel) detected GST-Msn5p but not Gsp1p, indicating that the interaction between the two proteins is very weak.

A number of studies have shown that Ran/Gsp1p-GTP bound to a β-karyopherin is not accessible to RanGAP/ Rna1p activation of its GTPase activity in vitro (Kutay *et al.*, 1997, 1998; Lounsbury and Macara, 1997; Hellmuth *et al.*, 1998). This enzymatic activity-based assay has been used to show the specific and cooperative formation of the Los1p, tRNA, Gsp1p-GTP export complex (Hellmuth *et al.*, 1998). Therefore, this assay was used to ascertain whether tRNA is an export cargo for Msn5p (Figure 14C). Incubation of
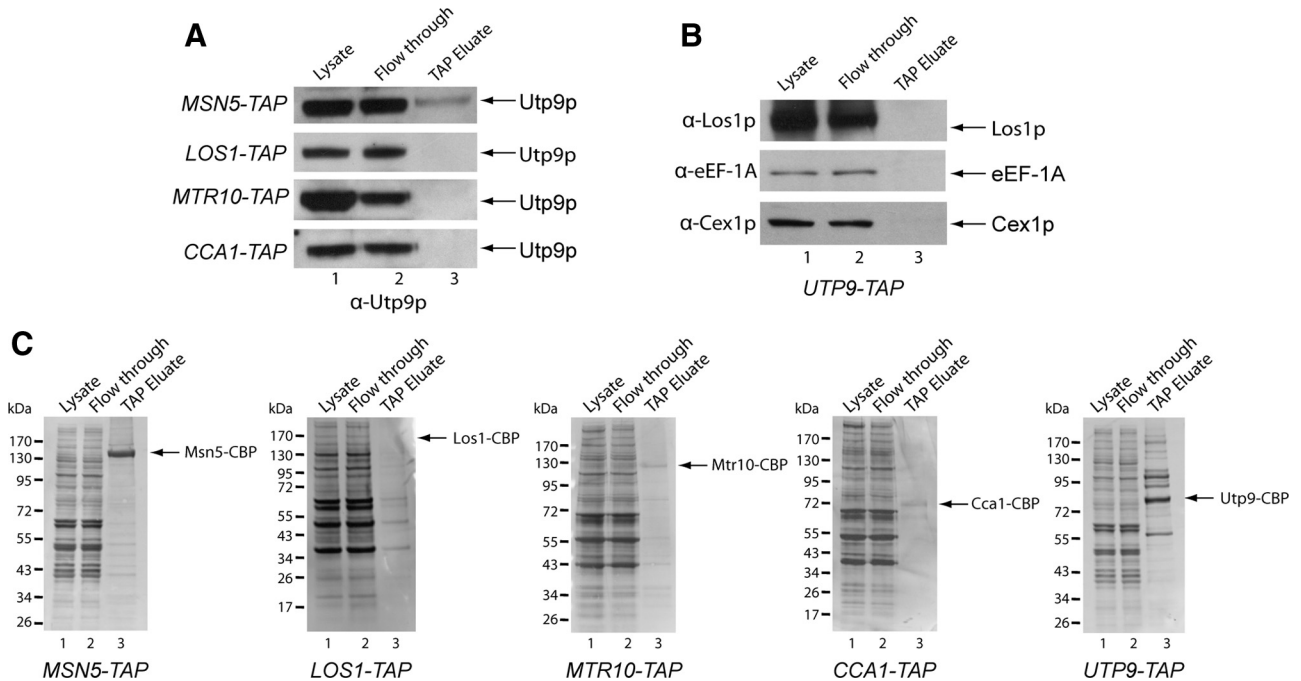
Figure 12. Utp9p copurifies with Msn5p but not with Los1p, Mtr10p, Cca1p, eEF-1A, or Cex1p. TAP was performed using cell extract from *MSN5-TAP, LOS1-TAP, MTR10-TAP, CCA1-TAP,* and *UTP9-TAP.* Total cell lysate (lane 1), the flow through from the IgG-Sepharose chromatography step (lane 2), and the eluate of proteins bound to calmodulin-Sepharose (lane 3) were subjected to Western blot analyses to detect Utp9p (A) and Los1p, eEF-1A, and Cex1p (B). The blots were then stained with SYPRO Ruby to detect copurifying proteins (C).

Gsp1p-GTP with Rna1p results in rapid GTP hydrolysis by Gsp1p. Similarly, the presence of Msn5p in the absence of tRNA did not significantly block Rna1p-induced Gsp1p GTP hydrolysis. However, the presence of Msn5p and aminoacylated or nonaminoacylated tRNA significantly reduced the rate of Rna1p-induced GTP hydrolysis by Gsp1p, indicating that Msn5p binds both forms of tRNA to about the same extent in a Gsp1p-GTP-dependent manner. These rates of GTP hydrolysis were slightly higher than that observed for Gsp1p alone. The data show that, like Los1p, binding of

tRNA to Msn5p is dependent on Gsp1p-GTP, validating that Msn5p is an authentic nuclear tRNA export receptor. Thus, the interaction observed between Utp9p and Msn5p in vitro and in vivo suggests that Utp9p may deliver retrograded tRNAs to Msn5p for export to the cytoplasm.

Utp8p has been shown previously to interact with Gsp1p in vivo and in vitro and to form a complex with Los1p and Gsp1p-GTP in a tRNA-dependent manner in vitro (Strub *et al.,* 2007). We therefore surmise that if Utp9p is delivering tRNA to Msn5p, it may interact with Gsp1p. To test this

Figure 13. Utp9p interacts directly and specifically with Msn5p. GST-Utp9p (100 µg, 1.1 nmol) was bound to GT-Sepharose in the presence (lane 3) or absence (lane 4) of 40 µM tRNA, and incubated with a twofold molar excess of Msn5p (319 µg, 2.2 nmol) (A). The same amount of Msn5p was incubated with bound GST (lane 5). GST-Los1p (100 µg, 800 pmol) was bound to GT-Sepharose in the presence (lane 3) or absence (lane 4) of 6 µM tRNA and incubated with a twofold molar excess of Utp9p (104 µg, 1.6 nmol) (B). The same amount of Utp9p was incubated with bound GST (lane 5). The resins were washed, and Utp9p and Los1p were released from bound GST using thrombin and TEV, respectively. Purified GST-Utp9p (A, lane 1), Msn5p (A, lane 2), Utp9p (B, lane 1), and GST-Los1p (B, lane 2), the bound proteins and unbound proteins in the wash eluates were subjected to Western blot analyses to detect Msn5p (A, top panels), GST-Utp9p (A, middle panel), Utp9p (B, top panels), and Los1p (B, middle panel). The blots were then stained with SYPRO Ruby to detect the proteins directly (A and B, bottom panels).
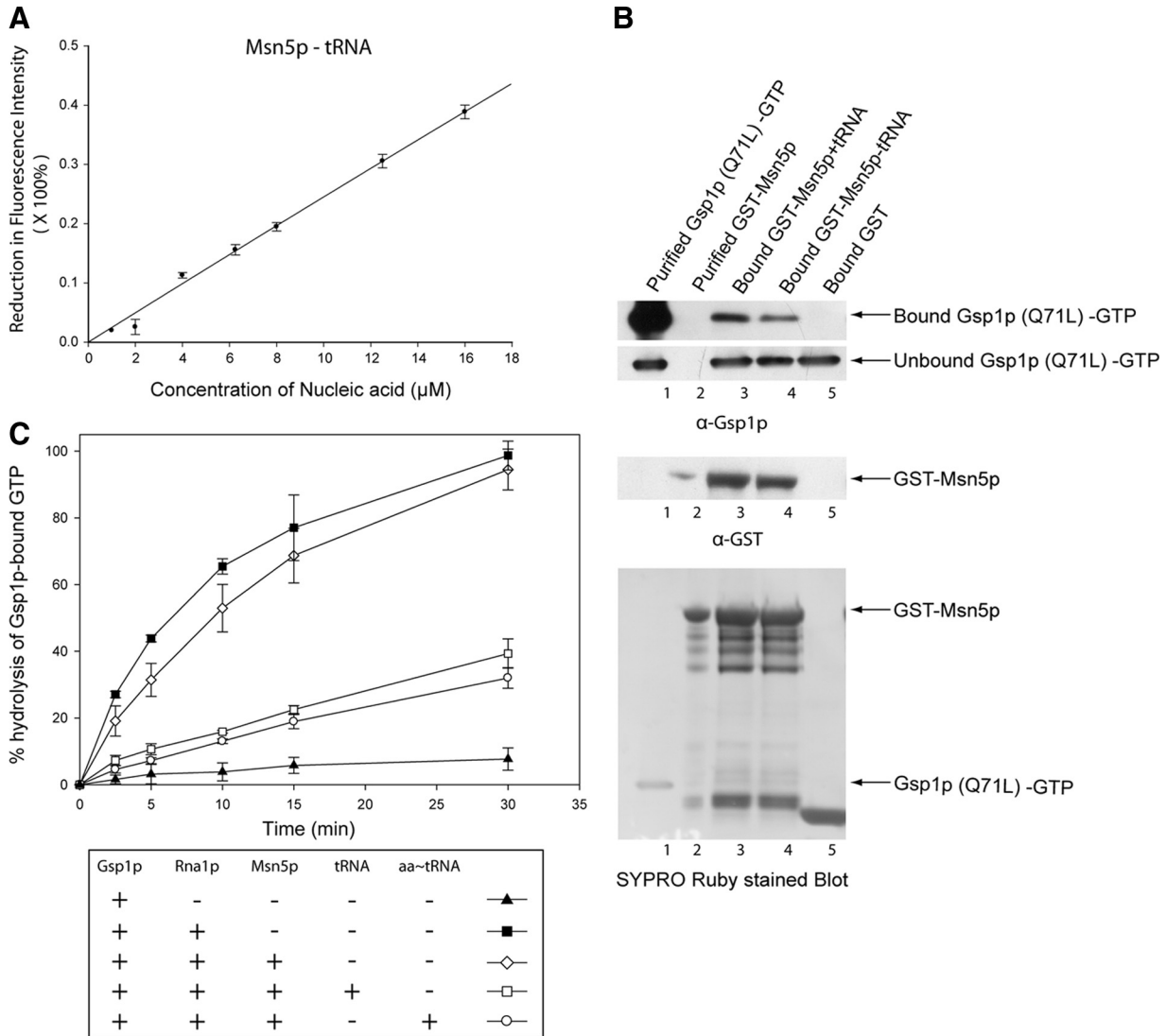
A

B

C
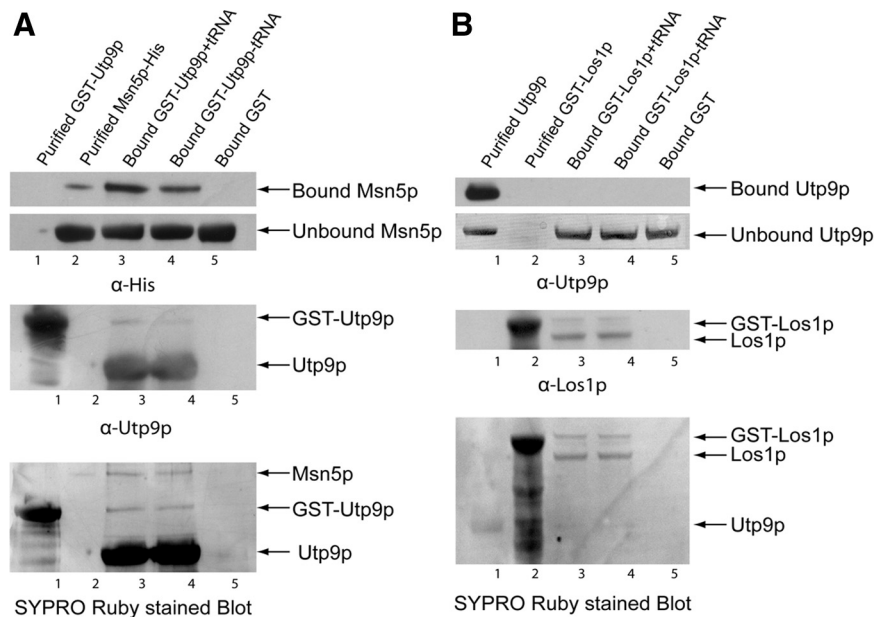
Figure 14. Loading of Msn5p with tRNA is dependent on Gsp1p. (A) Determination of the affinity of Msn5p for tRNA. Substrate-induced intrinsic fluorescence quenching of Trp residues was used to determine the tRNA binding affinity of Msn5p. (B) Interaction of Msn5p with Gsp1p in vitro is not dependent on tRNA. GST-Msn5p (100 μg, 0.7 nmol) was bound to GT-Sepharose in the presence (lane 3) or absence (lane 4) of 40 μM tRNA and incubated with a twofold molar excess of Gsp1p (Q71L)-GTP (35 μg, 1.4 nmol). The same amount of Gsp1p was incubated with bound GST (lane 5). The resins were washed and GST-Msn5p was released using 10 mM reduced glutathione. Purified Gsp1p (Q71L) (lane 1) and GST-Msn5p (lane 2), the bound proteins, and unbound Gsp1p in the wash eluates were subjected to Western blot analyses to detect Gsp1p (Q71L) (top panels) and GST-Msn5p (middle panel). SYPRO Ruby staining was performed on the membrane to detect the proteins directly (bottom panel). (C) Msn5p binds tRNA in a Gsp1p-dependent manner in a Gsp1p GTPase protection assay. The assays were performed in 350 μl of PBSM buffer. Gsp1 [γ-^{32}P]-GTP (5 pmol) was incubated with 0.5 μM Msn5p ($\diamond$), 0.5 μM Msn5p and 2.5 μM tRNA($\square$), or 0.5 μM Msn5p and 2.5 μM aminoacylated tRNA ($\bigcirc$) for 10 min, and Rna1p was added to a final concentration of 0.2 nM. Gsp1p [γ-^{32}P]-GTP (5 pmol) was incubated in the absence ($\blacktriangle$) or presence ($\blacksquare$) of 0.2 nM Rna1p. At the times specified, 50-μl aliquots were diluted into 200 μl of 20 mM phosphoric acid containing 5% (wt/vol) activated charcoal. The reactions were then centrifuged at maximum speed for 10 min in 1.5-ml tubes, and 100-μl aliquots were removed for scintillation counting to determine the amount of GTP hydrolyzed.

possibility, TAP was performed using extract prepared from *UTP9-TAP* or *UTP21-TAP* followed by Western blot analysis to detect Gsp1p (Figure 15A). Gsp1p was detected in the cell lysate (lane 1) and flow-through from IgG-Sepharose (lane 2). In addition, Gsp1p was found to copurify with Utp9p but not with Utp21p (lane 3). SYPRO Ruby staining of the blots shows the proteins that copurify with Utp9p and Utp21p (panel B). The data suggest that the association between Utp9p and Gsp1p in vivo is specific.

Protein-binding analyses were conducted in vitro to ascertain whether Utp9p interacts directly with Gsp1p (Figure 15C). GST-Utp9p bound to GT-Sepharose was incubated

with (lane 3) or without (lane 4) tRNA and with a twofold molar excess of Gsp1p (Q71L) loaded with GTP. Bound GST was incubated with the same amount of Gsp1p (Q71L; lane 5). The resins were washed and incubated with glutathione to release Utp9p. Purified Gsp1p (Q71L; lane 1) and GST-Utp9p (lane 2), the bound proteins and unbound Gsp1p (Q71L) in the wash eluates were subjected to Western blot analysis to detect Gsp1p (top panels) and Utp9p (middle panel). Gsp1p (Q71L) interacts with Utp9p in the presence (lane 3) or absence (lane 4) of tRNA, and a small amount of Gsp1p (Q71L) was found to interact with GST (lane 5). However, densitometric analyses of the blots indicate that
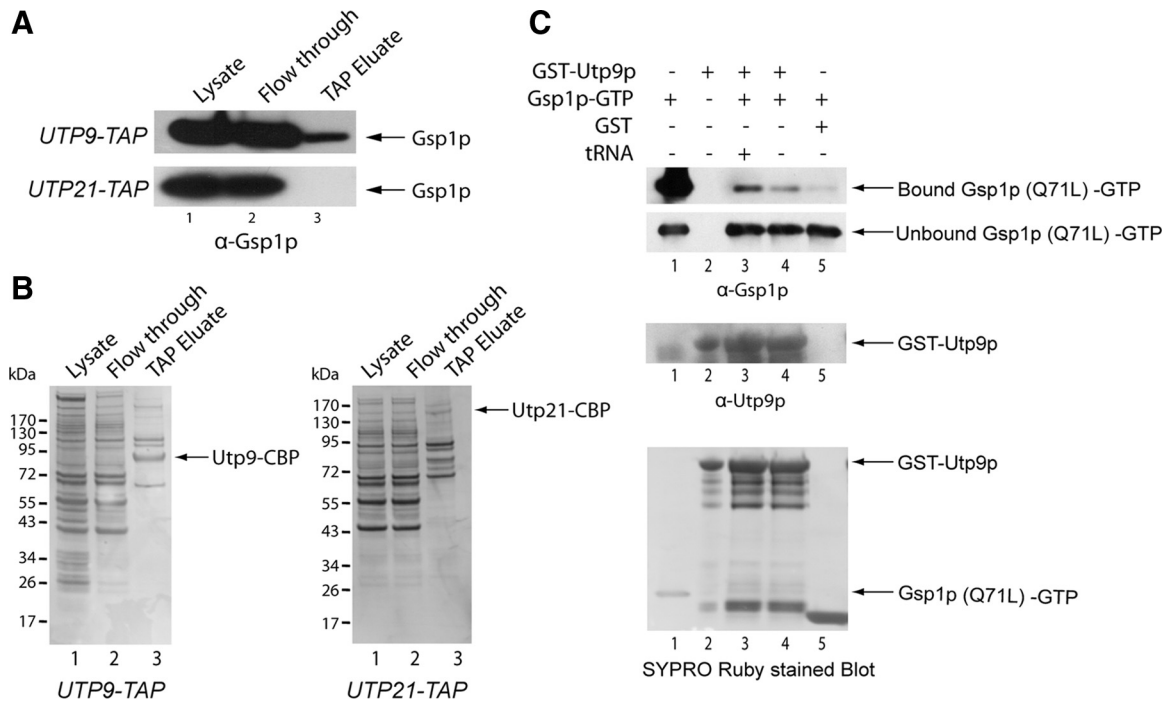
Figure 15. Utp9p interacts directly with Gsp1p in a tRNA-dependent manner. TAP was performed using cell extract from *UTP9-TAP* and *UTP21-TAP*. Total cell lysate (lane 1), the flow through from the IgG-Sepharose chromatography step (lane 2), and the eluate of proteins bound to calmodulin-Sepharose (lane 3) were subjected to Western blot analyses to detect Gsp1p (A). The blots were then stained with SYPRO Ruby to detect proteins that copurified with Utp9p and Utp21p (B). To ascertain whether Utp9p interacts directly with Gsp1p, protein-binding analyses were conducted in vitro (C). GST-Utp9p (100 μg, 1.1 nmol) bound to GT-Sepharose in the presence (lane 3) or absence (lane 4) of 40 μM tRNA was incubated with a twofold molar excess (55 μg, 2.2 nmol) of Gsp1p (Q71L) in the GTP bound form. The same amount of Gsp1p (Q71L)-GTP was incubated with bound GST (lane 5). The resins were washed and incubated with 10 mM reduced glutathione to release GST-Utp9p. Purified Gsp1p (Q71L) (lane 1) and GST-Utp9p (lane 2), the bound proteins, and Gsp1p in the wash eluates were subjected to Western blot analyses to detect Gsp1p (top panels) and GST-Utp9p (middle panel). The blot was then stained with SYPRO Ruby to detect the protein directly (bottom panel).

the amount of Gsp1p (Q71L) bound to Utp9p in the presence of tRNA was twofold higher compared with that bound to Utp9p in the absence of tRNA (cf. lanes 3 and 4). The data show that Utp9p interacts directly with Gsp1p, and that this interaction is dependent on tRNA. SYPRO Ruby staining of the blot detected GST-Utp9p but not Gsp1p, indicating that the interaction between the two proteins is very weak (bottom panel).

Utp9p Plays a Key Role in the Formation of the Msn5p-tRNA-Gsp1p-GTP Export Complex

The findings that Utp9p interacts directly with tRNA, Msn5p and Gsp1p in vitro and that Utp8p interacts with Msn5p and Utp9p in vivo and in vitro suggest that in vivo Utp9p and Utp8p may participate in the formation of the Msn5p-tRNA-Gsp1p-GTP export complex. To test this possibility, sequential protein-binding analyses were conducted to ascertain whether Utp8p (Figure 16A) or Utp9p (Figure 16B) forms a complex with Msn5p and Gsp1p-GTP in a tRNA-dependent manner. To determine whether Utp8p forms a complex with Msn5p and Gsp1p, GST-Utp8p bound to GT-Sepharose in the presence (lanes 1 and 3) or absence (lanes 2 and 4) of tRNA was incubated with a twofold molar excess of Msn5p (lanes 1 and 2) or Gsp1p (Q71L) loaded with GTP (lanes 3 and 4). The resins were washed and incubated with a twofold molar excess of Gsp1p (Q71L)-GTP (lanes 1 and 2) or Msn5p (lanes 3 and 4). Bound GST was incubated with the same amount of Msn5p (lane 5) or Gsp1p (Q71L; lane 6). The resins were washed and Utp8p

was released using TEV. The bound proteins and unbound Gsp1p (Q71L) and Msn5p in the wash eluates were subjected to Western blot analyses to detect Gsp1p (top panels), Msn5p (middle panels) and Utp8p (bottom panel). Msn5p and Gsp1p (Q71L) bound to Utp8p to the same extent in the presence (lanes 1 and 3) or absence (lanes 2 and 4) of tRNA irrespective of the order of addition of Msn5p and Gsp1p. A small amount of Gsp1p (Q71L) bound to GST (lane 6), but no binding was observed between Msn5p and GST (lane 5). The data show that Utp8p, Msn5p, and Gsp1p form a complex in a tRNA-independent manner.

Sequential binding analyses were conducted to determine whether Utp9p forms a complex with Msn5p and Gsp1p (Figure 16B). GST-Utp9p bound to GT-Sepharose in the presence (lanes 1 and 3) or absence (lanes 2 and 4) of tRNA was incubated with a twofold molar excess of Msn5p (lanes 1 and 2) or Gsp1p (Q71L)-GTP (lanes 3 and 4). The resins were washed and incubated with a twofold molar excess of Gsp1p (Q71L)-GTP (lanes 1 and 2) or Msn5p (lanes 3 and 4). Bound GST was incubated with same amount of Msn5p (lane 5) or Gsp1p (Q71L; lane 6). The resins were washed and Utp9p was released using thrombin. The bound proteins and unbound Msn5p and Gsp1p (Q71L) in the wash eluates were subjected to Western blot analyses to detect Gsp1p (top panels), Msn5p (middle panels) and Utp9p (bottom panel). The same amount of Msn5p bound to Utp9p in the presence or absence of tRNA and irrespective of the order of addition of Msn5p and Gsp1p. In contrast, a larger amount of Gsp1p (Q71L)-GTP bound to Utp9p in the pres-
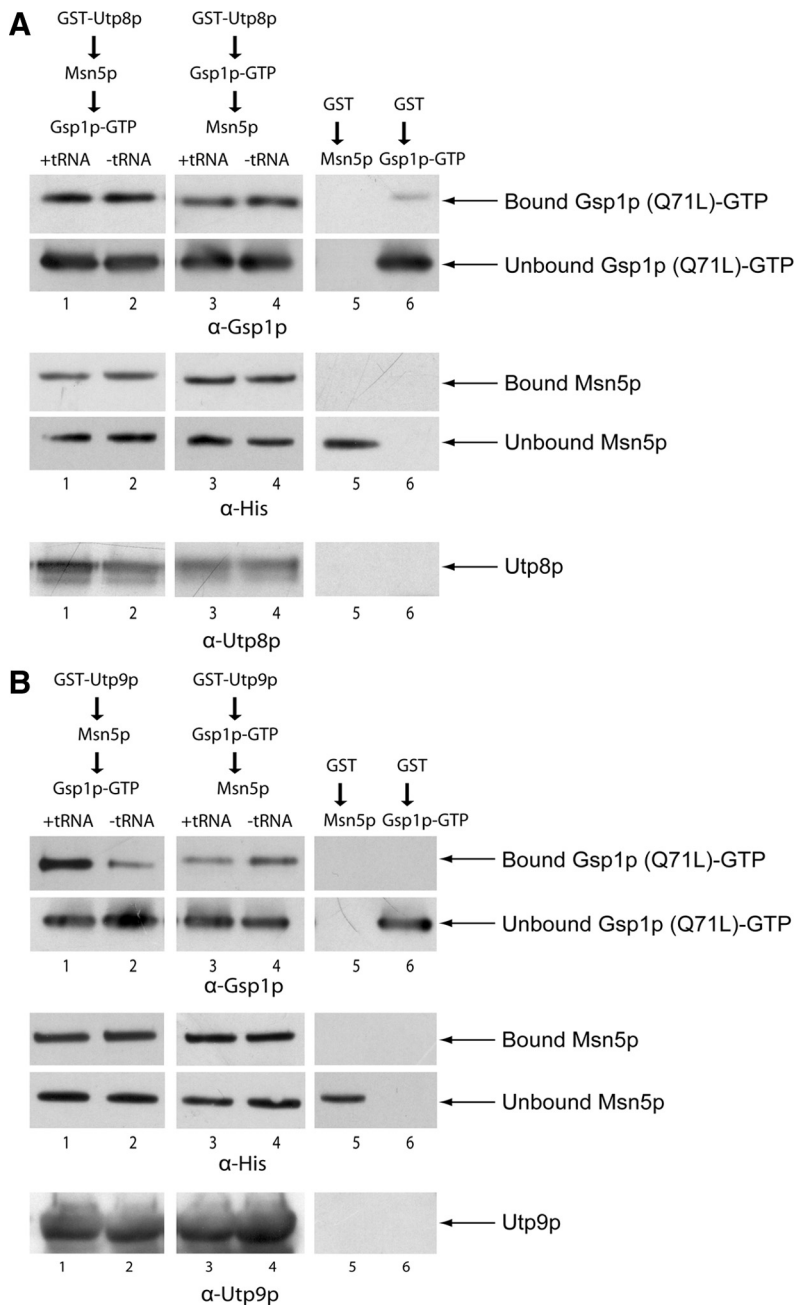
Figure 16. Utp9p plays a more important role than Utp8p in the assembly of the Msn5p-tRNA-Gsp1p-GTP export complex. (A) Utp8p forms a complex with Gsp1p and Msn5p in a tRNA-independent manner. GST-Utp8p (100 μg, 1 nmol) bound to GT-Sepharose was incubated with (lanes 1 and 3) or without (lanes 2 and 4) 6 μM tRNA. The resins were washed and incubated with a twofold molar excess of Msn5p (284 μg, 2 nmol; lanes 1 and 2) or Gsp1p (Q71L)-GTP (50 μg, 2 nmol; lanes 3 and 4). The resins were washed and incubated with a twofold molar excess of Gsp1p (Q71L)-GTP (50 μg, 2 nmol; lanes 1 and 2) or Msn5p (284 μg, 2 nmol; lanes 3 and 4). Bound GST was incubated with the same amount of Msn5p (lane 5) or Gsp1p (Q71L) (lane 6). Utp8p was released from the washed resins using TEV, and the bound proteins and unbound proteins in the washes were subjected to Western blot analysis to detect Gsp1p (top panels), Msn5p (middle panels), and Utp8p (bottom panel). (B) Formation of a complex between Utp9p, Msn5p, and Gsp1p is dependent on tRNA and the order of addition of the interacting proteins. GST-Utp9p (100 μg, 1.11 nmol) bound to GT-Sepharose was incubated with (lanes 1 and 3) or without (lanes 2 and 4) 40 μM tRNA. The resins were washed and incubated with a twofold molar excess of Msn5p (312 μg, 2.2 nmol; lanes 1 and 2) or Gsp1p (Q71L)-GTP (55 μg, 2.2 nmol; lanes 3 and 4). The resins were washed and incubated with a twofold molar excess of Gsp1p (Q71L)-GTP (55 μg, 2.2 nmol; lanes 1 and 2) or Msn5p (312 μg, 2.2 nmol; lanes 3 and 4). The same amount of Msn5p (lane 5) or Gsp1p (Q71L) (lane 6) was incubated with bound GST. Utp9p was released from the washed resins using thrombin. The bound proteins and unbound proteins in the wash eluates were analyzed for Gsp1p (Q71L) (top panels), Msn5p (middle panels), and Utp9p (bottom panel) by Western blot analyses.

ence than in the absence of tRNA when Msn5p was added first (cf. lanes 1 and 2). The amount of Gsp1p bound to Utp9p in the presence of tRNA when it was added after Msn5p (lane 1) was fourfold higher than that observed in the absence of tRNA (lane 2). In contrast, Gsp1p interacted with Utp9p to the same extent in the presence or absence of tRNA when it was added before Msn5p (cf. lanes 3 and 4). Both Msn5p (lane 5) and Gsp1p (Q71L; lane 6) did not interact with GST alone. The data suggest that Utp9p is playing a more important role than Utp8p in the formation of the tRNA export complex.

DISCUSSION

A small percentage of eukaryotic tRNA genes contain an intron, and recent studies have demonstrated that removal of the intron from the pre-tRNA transcript occurs in the cytoplasm of *S. cerevisiae* (Yoshihisa *et al.*, 2003, 2007). Furthermore, it has been shown that the spliced tRNAs then undergo retrograde transport from the cytoplasm to the nucleus (Shaheen and Hopper, 2005; Takano *et al.*, 2005), followed by reexport to the cytoplasm after quality assurance by aminoacylation in the nucleolus. However, retrograded tRNAs have been shown to accumulate in the nucleus of *S. cerevisiae* deprived of glucose, nitrogen, amino acids, or phosphate (Shaheen and Hopper, 2005; Shaheen *et al.*, 2007; Hurto *et al.*, 2007; Whitney *et al.*, 2007). This appears to occur because of a block at a step specifically involved in nuclear reexport of retrograded tRNAs, as nuclear accumulation of tRNA[Tyr] (Figure 8) and tRNA[Leu] (Supplemental Figure S8) made from intron-containing pre-tRNAs, but not tRNA[Gly] (Figure 8) and tRNA[His] (Supplemental Figure S8),

which are tRNAs derived from intronless pre-tRNAs, was observed in *S. cerevisiae* starved of amino acids or nitrogen. It is possible that inhibition of nuclear reexport of retrograded tRNAs occurs after the nuclear tRNA aminoacylation quality assurance step, as retrograded tRNAs are found in the aminoacylated form (Whitney *et al.,* 2007). Importantly, these data imply that separate pathways are used for nuclear reexport of retrograded tRNAs and nonretrograded tRNAs, which are tRNAs derived from intronless pre-tRNAs and are matured in the nucleus.

Although the mechanism responsible for nuclear reexport of retrograded tRNAs is not understood, several lines of evidence obtained by this study suggest that Utp9p is an intranuclear component of this pathway that acts at a step after the tRNAs have undergone maturation and aminoacylation in the nucleus. 1) Depletion of Utp9p affects nuclear export of mature tRNAs derived from intron-containing pre-tRNAs but not tRNAs made from intronless precursors (Figures 6 and 7). 2) Amino acid or nitrogen starvation results in nuclear accumulation of tRNAs made from intron-containing pre-tRNAs but not tRNAs made from intronless precursors (Figures 8 and S8). 3) Loss of the function of Utp9p did not affect splicing or nuclear aminoacylation of a tRNA derived from intron-containing precursor (Figures S6 and S7). 4) Nutrient deprivation of Utp9p-depleted cells did not abolish nuclear accumulation of tRNA$^{\text{Tyr}}$ (data not shown). 5) Utp9p does not function as a nuclear tRNA export receptor or an adaptor protein for a nuclear tRNA export receptor, because it does not shuttle between the nucleus and cytoplasm (Figure 10A). In addition, the finding that Utp8p interacts with Utp9p in vivo and in vitro suggests that Utp8p is an intranuclear component that is required for nuclear reexport of retrograded tRNAs (Figure 11); however, it also participates in the pathway that is involved in nuclear export of mature tRNAs derived from intronless precursors, as depletion of Utp8p blocks export of mature tRNAs obtained from both classes of pre-tRNAs (Steiner-Mosonyi *et al.,* 2003). Furthermore, Msn5p appears to be one of the export receptors that facilitate nuclear export of retrograded tRNAs based on in vivo and in vitro data showing that it interacts with Utp9p (Figures 12, 13, and 16). The cytoplasmic Cex1p may also participate in this pathway to collect aminoacylated retrograded tRNAs from the export receptor, because it was found to copurify with Msn5p by TAP (McGuire and Mangroo, 2007). However, it is unlikely that Utp9p, Utp8p, Msn5p, and Cex1p are the only proteins involved in the nuclear tRNA reexport pathway, because the functions of Msn5p and Cex1p are not essential.

Utp8p has been shown to collect aminoacyl-tRNAs from the aminoacyl-tRNA synthetases and translocate them from the nucleolus to the nuclear tRNA export receptors located in the nucleoplasm and NPC by using a channelling mechanism (Strub *et al.,* 2007). Like Utp8p (Steiner-Mosonyi *et al.,* 2003), Utp9p binds tRNA directly and saturably in vitro (Figure 9A). Furthermore, Utp9p copurifies with Utp8p by TAP and interacts directly with Utp8p in vitro (Figure 11, A and B). However, unlike Utp8p (Strub *et al.,* 2007), Utp9p does not appear to interact with aminoacyl-tRNA synthetases in vivo, as it does not interact with the tyrosyl-tRNA synthetase in vivo and in vitro (Figure 11A and Supplemental Figure S9). An interpretation that is consistent with the data is that Utp9p does not facilitate transfer of aminoacylated retrograded tRNAs from the aminoacyl-tRNA synthetases to Utp8p. Instead, it most likely acts in concert with Utp8p to translocate the tRNAs from the nucleolus to a nuclear tRNA export receptor of a pathway specific for nuclear reexport of retrograded tRNAs. However, it is not known how Utp9p discriminates between retrograded tRNAs derived from intron-containing precursors and non-retrograded tRNAs made from intronless precursors. The finding that the interaction between Utp8p and Utp9p in vitro is not dependent on tRNA suggests that in vivo an unidentified protein may recruit Utp9p to Utp8p carrying aminoacylated retrograded tRNA or that a protein transfers aminoacylated retrograded tRNAs from the synthetases to Utp9p, followed by recruitment of Utp8p for translocation of the Utp9p-tRNA complex to the nuclear export receptor of the nuclear tRNA reexport pathway.

Los1p has been unambiguously demonstrated to be a nuclear tRNA export receptor (Hellmuth *et al.,* 1998). In contrast, Msn5p was presumed to be involved in translocation of tRNAs across the NPC based on the finding that an *msn5 los1* strain, which is not affected in growth, exhibits a reduction in the efficiency of nuclear export of tRNA (Takano *et al.,* 2005). Because Msn5p also functions as a nuclear import receptor for proteins (Quan *et al.,* 2006), it is possible that the reduced efficiency of nuclear tRNA export observed in the *msn5 los1* strain could be due to a defect in nuclear import of a protein that plays a redundant role in the nuclear tRNA export process. We established biochemically that tRNA is a poor substrate for Msn5p in the absence of Gsp1p-GTP (Figure 14, A and C), but like other nuclear export receptors including Los1p, Msn5p binding to tRNA requires Gsp1p-GTP (Figure 14C), suggesting that Msn5p also functions as a nuclear tRNA export receptor. This notion is consistent with in vitro and in vivo studies showing that Msn5p interacts with Utp8p and Cex1p (McGuire and Mangroo, 2007; Strub *et al.,* 2007). Msn5p may export both aminoacylated and nonaminoacylated tRNA, because it can bind both forms of tRNA in a Gsp1p-GTP-dependent manner (Figure 14C). Moreover, the finding that Utp9p interacts with Msn5p but not with Los1p in vivo and in vitro (Figures 12 and 13) suggests that Msn5p facilitates reexport of retrograded tRNAs from the nucleus to the cytoplasm. However, it is unlikely that Msn5p is the only receptor responsible for nuclear reexport of retrograded tRNAs, as the loss of Msn5p function does not affect the efficiency of nuclear export of tRNAs derived from intron-containing pre-tRNAs or cell growth (data not shown). It is possible that an unidentified export receptor also participates in nuclear export of retrograded tRNAs. Utp9p may also function with this nuclear export receptor, because loss of Utp9p function has a more prominent impact on nuclear reexport of retrograded tRNA than the loss of Msn5p function alone. The finding that Utp9p is not required for Los1p-mediated nuclear tRNA export does not exclude the possibility that Los1p can facilitate nuclear reexport of retrograded tRNAs.

Previous studies have shown that Utp8p loaded with tRNA, Los1p, and Gsp1p form a complex. However, this complex is not formed when Utp8p lacks tRNA, and the tRNA-dependent formation of the complex only occurs when Los1p is added to Utp8p containing tRNA followed by addition of Gsp1p-GTP (Strub *et al.,* 2007). These results led to the suggestion that Utp8p facilitates the formation of the Los1p-tRNA-Gsp1p-GTP export complex. We found that Utp9p copurifies with Msn5p and Gsp1p by TAP (Figures 12A and 15A). Utp9p also interacts directly with Msn5p and Gsp1p in vitro (Figures 13A and 15C). We therefore surmise that Utp8p and Utp9p may be required for formation of the Msn5p-tRNA-Gsp1p-GTP export complex in vivo. Measurement of the protection of the Rna1p-induced GTPase activity of Gsp1p demonstrates that in vitro formation of the Msn5p-tRNA-Gsp1p-GTP complex can occur without the assistance of additional factors (Figure 14C). Furthermore, by using

this enzymatic assay we could not detect any effect of Utp8p and Utp9p on the efficiency of complex formation (data not shown). However, in vitro protein-binding analyses indicate that Utp8p, Msn5p, and Gsp1p form a complex that was not dependent on tRNA or the order of addition of Msn5p and Gsp1p to Utp8p (Figure 16A). In contrast, Gsp1p was found to interact with Msn5p and Utp9p in a tRNA-dependent manner when Msn5p was added first to the Utp9p-tRNA complex, but not when it was added to the Utp9p-tRNA complex before the addition of Msn5p (Figure 16B). Based on the finding from in vitro protein-binding analyses that the interaction between Msn5p and Gsp1p was not dependent on tRNA, and the binding between Utp9p and Gsp1p was tRNA-dependent (Figure 15) suggest that the tRNA-dependency of binding of Gsp1p to the Msn5p-Utp9p-tRNA complex is most likely related to Utp9p. Taken together, the data suggest that both Utp8p and Utp9p are involved in formation of the export complex in vivo. However, Utp9p appears to play a more important role than Utp8p in the assembly of the export complex. Utp9p bound to tRNA may, in part, facilitate binding of Gsp1p-GTP to Msn5p. A model that is consistent with the data suggests that both Utp8p and Utp9p bound to tRNA interact with Msn5p to indicate the presence of tRNA; Utp9p interacts with Gsp1p-GTP to re-cruit it to Msn5p, allowing Msn5p to interact with the tRNA. Gsp1p then interacts with Utp8p to facilitate release of the tRNA, and dissociation of the Utp8p-Utp9p complex. How-ever, further studies are required to fully understand the mechanism of Utp8p- and Utp9p-mediated loading of Msn5p with tRNA, and the significance of the interaction of Gsp1p with Utp8p and Utp9p.

We have shown that Utp9p and Msn5p are components of a pathway that facilitates reexport of retrograded tRNAs from the nucleus to the cytoplasm in *S. cerevisiae*. Further-more, the results suggest that Utp9p acts in concert with Utp8p to translocate aminoacylated retrograded tRNAs from the nucleolus to the tRNA export receptor Msn5p and assist with the formation of the Msn5p-tRNA-Gsp1p-GTP export complex. Why nuclear export of retrograded tRNAs should involve a pathway that is different from that required for nuclear export of nonretrograded tRNAs is not under-stood. Furthermore, the significance of the involvement of Utp9p in both transcription of rRNA gene and nuclear re-export of retrograded tRNA is not understood. A possible explanation is that Utp9p also plays a regulatory role that coordinates nuclear reexport of retrograded tRNA and ribo-some biogenesis in the nucleus. This communication be-tween the two processes may be important for controlling the protein translation rate, which is dictated by a number of external stimuli such as nutrient availability. This hypothe-sis is consistent with the finding that both nuclear reexport of retrograded tRNAs (Shaheen and Hopper, 2005; Shaheen *et al.*, 2007; Whitney *et al.*, 2007) and ribosome biogenesis are affected by nutrient-related stress (Jorgensen and Tyers, 2004; Li *et al.*, 2006; Zaman *et al.*, 2008).

ACKNOWLEDGMENTS

REFERENCES

Arts, G. J., Fornerod, M., and Mattaj, I. W. (1998). Identification of a nuclear export receptor for tRNA. Curr. Biol. *8*, 305–314.

Azad, A. K., Stanford, D. R., Sarkar, S., and Hopper, A. K. (2001). Role of nuclear pools of aminoacyl-tRNA synthetases in tRNA nuclear export. Mol. Biol. Cell *12*, 1381–1392.

Ben-Aroya, S., Coombes, C., Kwok, T., O'Donnell, K. A., Boeke, J. D., and Hieter, P. (2008). Toward a comprehensive temperature-sensitive mutant repository of the essential genes of *Saccharomyces cerevisiae*. Mol. Cell *30*, 248–258.

Bischoff, F. R., Klebe, C., Kretschmer, J., Wittinghofer, A., and Ponstingl, H. (1994). Rangap1 induced Gtpase activity of nuclear Ras-related Ran. Proc. Natl. Acad. Sci. USA *91*, 2587–2591.

Bischoff, F. R., Krebber, H., Smirnova, E., Dong, W. H., and Ponstingl, H. (1995). Coactivation of Rangtpase and Inhibition of Gtp dissociation by Ran Gtp-binding protein Ranbp1. EMBO J. *14*, 705–715.

Bohnsack, M. T., Regener, K., Schwappach, B., Saffrich, R., Paraskeva, E., Hartmann, E., and Gorlich, D. (2002). Exp5 exports eEF1A via tRNA from nuclei and synergizes with other transport pathways to confine translation to the cytoplasm. EMBO J. *21*, 6205–6215.

Calado, A., Treichel, N., Muller, E. C., Otto, A., and Kutay, U. (2002). Expor-tin-5-mediated nuclear export of eukaryotic elongation factor 1A and tRNA. EMBO J. *21*, 6216–6224.

Cleary, J. D., and Mangroo, D. (2000). Nucleotides of the tRNA D-stem that play an important role in nuclear-tRNA export in *Saccharomyces cerevisiae*. Biochem. J. *347*(Pt 1), 115–122.

Dilworth, D. J., Suprapto, A., Padovan, J. C., Chait, B. T., Wozniak, R. W., Rout, M. P., and Aitchison, J. D. (2001). Nup2p dynamically associates with the distal regions of the yeast nuclear pore complex. J. Cell Biol. *153*, 1465–1478.

Dragon, F., *et al.* (2002). A large nucleolar U3 ribonucleoprotein required for 18S ribosomal RNA biogenesis. Nature *417*, 967–970.

Englert, M., Latz, A., Becker, D., Gimple, O., Beier, H., and Akama, K. (2007). Plant pre-tRNA splicing enzymes are targeted to multiple cellular compart-ments. Biochimie *89*, 1351–1365.

Ernens, I., Goodfellow, S. J., Innes, F., Kenneth, N. S., Derblay, L. E., White, R. J., and Scott, P. H. (2006). Hypoxic stress suppresses RNA polymerase III recruitment and tRNA gene transcription in cardiomyocytes. Nucleic Acids Res. *34*, 286–294.

Gadal, O., Strauss, D., Kessl, J., Trumpower, B., Tollervey, D., and Hurt, E. (2001). Nuclear export of 60s ribosomal subunits depends on Xpo1p and requires a nuclear export sequence-containing factor, Nmd3p, that associates with the large subunit protein Rpl10p. Mol. Cell. Biol. *21*, 3405–3415.

Gallagher, J.E.G., Dunbar, D. A., Granneman, S., Mitchell, B. M., Osheim, Y., Beyer, A. L., and Baserga, S. J. (2004). RNA polymerase I transcription and pre-rRNA processing are linked by specific SSU processome components. Genes Dev. *18*, 2506–2517.

Ghavidel, A., Kislinger, T., Pogoutse, O., Sopko, R., Jurisica, I., and Emili, A. (2007). Impaired tRNA nuclear export links DNA damage and cell-cycle checkpoint. Cell *131*, 915–926.

Giaever, G., *et al.* (2002). Functional profiling of the *Saccharomyces cerevisiae* genome. Nature *418*, 387–391.

Gite, S., and RajBhandary, U. L. (1997). Lysine 207 as the site of cross-linking between the 3'-end of *Escherichia coli* initiator tRNA and methionyl-tRNA formyltransferase. J. Biol. Chem. *272*, 5305–5312.

Grosshans, H., Hurt, E., and Simos, G. (2000). An aminoacylation-dependent nuclear tRNA export pathway in yeast. Genes Dev. *14*, 830–840.

Hellmuth, K., Lau, D. M., Bischoff, F. R., Kunzler, M., Hurt, E., and Simos, G. (1998). Yeast Los1p has properties of an exportin-like nucleocytoplasmic transport factor for tRNA. Mol. Cell. Biol. *18*, 6374–6386.

Hopper, A. K., and Phizicky, E. M. (2003). tRNA transfers to the limelight. Genes Dev. *17*, 162–180.

Huh, W. K., Falvo, J. V., Gerke, L. C., Carroll, A. S., Howson, R. W., Weissman, J. S., and O'Shea, E. K. (2003). Global analysis of protein localization in budding yeast. Nature *425*, 686–691.

Hurto, R. L., Tong, A.H.Y., Boone, C., and Hopper, A. K. (2007). Inorganic phosphate deprivation causes tRNA nuclear accumulation via retrograde transport in *Saccharomyces cerevisiae*. Genetics *176*, 841–852.

Jorgensen, P., and Tyers, M. (2004). How cells coordinate growth and divi-sion. Curr. Biol. *14*, R1014–R1027.

Kanemaki, M., Sanchez-Diaz, A., Gambus, A., and Labib, K. (2003). Functional proteomic identification of DNA replication proteins by induced proteolysis in vivo. Nature *423*, 720–724.

Krogan, N. J., *et al.* (2004). High-definition macromolecular composition of yeast RNA-processing complexes. Mol. Cell *13*, 225–239.

Kruse, C., Willkomm, D. K., Grunweller, A., Vollbrandt, T., Sommer, S., Busch, S., Pfeiffer, T., Brinkmann, J., Hartmann, R. K., and Muller, P. K. (2000). Export and transport of tRNA are coupled to a multi-protein complex. Biochemical J. *346*, 107–115.

Kutay, U., Bischoff, F. R., Kostka, S., Kraft, R., and Gorlich, D. (1997). Export of importin alpha from the nucleus is mediated by a specific nuclear transport factor. Cell *90*, 1061–1071.

Kutay, U., Lipowsky, G., Izaurralde, E., Bischoff, F. R., Schwarzmaier, P., Hartmann, E., and Gorlich, D. (1998). Identification of a tRNA-specific nuclear export receptor. Mol. Cell *1*, 359–369.

Li, H., Tsang, C. K., Watkins, M., Bertram, P. G., and Zheng, X.F.S. (2006). Nutrient regulates Tor1 nuclear localization and association with rDNA promoter. Nature *442*, 1058–1061.

Lounsbury, K. M., and Macara, I. G. (1997). Ran-binding protein 1 (RanBP1) forms a ternary complex with Ran and karyopherin beta and reduces Ran GTPase-activating protein (RanGAP) inhibition by karyopherin beta. J. Biol. Chem. *272*, 551–555.

Lund, E., and Dahlberg, J. E. (1998). Proofreading and aminoacylation of tRNAs before export from the nucleus. Science *282*, 2082–2085.

Maurer, P., Redd, M., Solsbacher, J., Bischoff, F. R., Greiner, M., Podtelejnikov, A. V., Mann, M., Stade, K., Weis, K., and Schlenstedt, G. (2001). The nuclear export receptor Xpo1p forms distinct complexes with NES transport substrates and the yeast ran binding protein 1 (Yrb1p). Mol. Biol. Cell *12*, 539–549.

McGuire, A. T., Keates, R.A.B., Cook, S., and Mangroo, D. (2009). Structural modeling identified the tRNA-binding domain of Utp8p, an essential nucleolar component of the nuclear tRNA export machinery of *Saccharomyces cerevisiae*. Biochem. Cell Biol. Biochim. Biol. Cell. *87*, 431–443.

McGuire, A. T., and Mangroo, D. (2007). Cex1p is a novel cytoplasmic component of the *Saccharomyces cerevisiae* nuclear tRNA export machinery. EMBO J. *26*, 288–300.

Paushkin, S. V., Patel, M., Furia, B. S., Peltz, S. W., and Trotta, C. R. (2004). Identification of a human endonuclease complex reveals a link between tRNA splicing and pre-mRNA 3′ end formation. Cell *117*, 311–321.

Puig, O., Caspary, F., Rigaut, G., Rutz, B., Bouveret, E., Bragado-Nilsson, E., Wilm, M., and Seraphin, B. (2001). The tandem affinity purification (TAP) method: a general procedure of protein complex purification. Methods *24*, 218–229.

Quan, X. X., Tsoulos, P., Kuritzky, A., Zhang, R., and Stochaj, U. (2006). The carrier Msn5p/Kap142p promotes nuclear export of the hsp70 Ssa4p and relocates in response to stress. Mol. Microbiol. *62*, 592–609.

Sarkar, S., Azad, A. K., and Hopper, A. K. (1999). Nuclear tRNA aminoacylation and its role in nuclear export of endogenous tRNAs in *Saccharomyces cerevisiae*. Proc. Natl. Acad. Sci. USA *96*, 14366–14371.

Schafer, T., Strauss, D., Petfalski, E., Tollervey, D., and Hurt, E. (2003). The path from nucleolar 90S to cytoplasmic 40S pre-ribosomes. EMBO J. *22*, 1370–1380.

Schmidt, W. M., *et al.* (2007). Mutation in the Scyl1 gene encoding aminoterminal kinase-like protein causes a recessive form of spinocerebellar neurodegeneration. EMBO Rep. *8*, 691–697.

Shaheen, H. H., and Hopper, A. K. (2005). Retrograde movement of tRNAs from the cytoplasm to the nucleus in *Saccharomyces cerevisiae*. Proc. Natl. Acad. Sci. USA *102*, 11290–11295.

Shaheen, H. H., Horetsky, R. L., Kimball, S. R., Murthi, A., Jefferson, L. S., and Hopper, A. K. (2007). Retrograde nuclear accumulation of cytoplasmic tRNA in rat hepatoma cells in response to amino acid deprivation. Proc. Natl. Acad. Sci. USA *104*, 8845–8850.

Stade, K., Ford, C. S., Guthrie, C., and Weis, K. (1997). Exportin 1 (Crm1p) is an essential nuclear export factor. Cell *90*, 1041–1050.

Steiner-Mosonyi, M., Leslie, D. M., Dehghani, H., Aitchison, J. D., and Mangroo, D. (2003). Utp8p is an essential intranuclear component of the nuclear tRNA export machinery of *Saccharomyces cerevisiae*. J. Biol. Chem. *278*, 32236–32245.

Steiner-Mosonyi, M., and Mangroo, D. (2004). The nuclear tRNA aminoacylation-dependent pathway may be the principal route used to export tRNA from the nucleus in *Saccharomyces cerevisiae*. Biochem. J. *378*, 809–816.

Strub, B. R., Eswara, M.B.K., Pierce, J. B., and Mangroo, D. (2007). Utp8p is a nucleolar tRNA-binding protein that forms a complex with components of the nuclear tRNA export machinery in *Saccharomyces cerevisiae*. Mol. Biol. Cell *18*, 3845–3859.

Takano, A., Endo, T., and Yoshihisa, T. (2005). tRNA actively shuttles between the nucleus and cytosol in yeast. Science *309*, 140–142.

Wang, C. C., and Schimmel, P. (1999). Species barrier to RNA recognition overcome with nonspecific RNA binding domains. J. Biol. Chem. *274*, 16508–16512.

White, R. J. (2004a). RNA polymerase III transcription—a battleground for tumour suppressors and oncogenes. Eur. J. Cancer *40*, 21–27.

White, R. J. (2004b). RNA polymerase III transcription and cancer. Oncogene *23*, 3208–3216.

Whitney, M. L., Hurto, R. L., Shaheen, H. H., and Hopper, A. K. (2007). Rapid and reversible nuclear accumulation of cytoplasmic tRNA in response to nutrient availability. Mol. Biol. Cell *18*, 2678–2686.

Yoshihisa, T., Ohshima, C., Yunoki-Esaki, K., and Endo, T. (2007). Cytoplasmic splicing of tRNA in *Saccharomyces cerevisiae*. Genes Cell. *12*, 285–297.

Yoshihisa, T., Yunoki-Esaki, K., Ohshima, C., Tanaka, N., and Endo, T. (2003). Possibility of cytoplasmic pre-tRNA splicing: the yeast tRNA splicing endonuclease mainly localizes on the mitochondria. Mol. Biol. Cell *14*, 3266–3279.

Zaitseva, L., Myers, R., and Fassati, A. (2006). tRNAs promote nuclear import of HIV-1 intracellular reverse transcription complexes. Plos Biol. *4*, 1689–1706.

Zaman, S., Lippman, S. I., Zhao, X., and Broach, J. R. (2008). How *Saccharomyces* Responds to Nutrients. Annu. Rev. Genet. *42*, 27–81.